Russian Journal of Earth Sciences Online ISSN: 1681-1208

Special Issue: "Kamchatka Earthquake M 8.8 on July 29, 2025"

The July 29, 2025 Kamchatka Earthquake, M_W 8.9: Examination Based on Regional Data Through End-2025

D. V. Chebrov[1,*], E. A. Matveenko[1], I. R. Abubakirov[1], D. V. Droznin[1], S. Ya. Droznina[1], A. V. Lander[2], S. V. Mityushkina[1], V. M. Pavlov[1], A. A. Raevskaya[1], S. L. Senyukov[1], and N. N. Titkov[1]

[1] Kamchatka Branch of the Geophysical Survey of the Russian Academy of Sciences (KB GS RAS), Petropavlovsk-Kamchatsky, Russian Federation

[2] Institute for Earthquake Prediction Theory and Mathematical Geophysics of the Russian Academy of Sciences, Moscow, Russian Federation

* **Correspondence to:** D. V. Chebrov, danila@emsd.ru

Abstract: This article presents data on the M_W 8.9 Kamchatka earthquake of July 29, 2025, compiled by the Kamchatka Branch of the Geophysical Survey of the Russian Academy of Sciences (KB GS RAS) as of December 31, 2025. The Kamchatka earthquake is one of the largest seismic events in the history of instrumental observations. To date it ranks as the sixth most powerful event ever recorded in the world. The rupture zone, estimated based on the aftershock area, is 580 × 180 km and roughly coincides with the source area of the Great Kamchatka Earthquake of November 4, 1952 (M_W 9.0). The 73-year gap between these two megathrust earthquakes that occurred approximately in the same area is significantly shorter than what would be expected from the widely accepted concepts of the seismic cycle. The article provides information on source parameters of the main shock, the operation of the Tsunami Warning Service, a catalog of aftershock mechanisms, the characteristics of strong ground motions caused by the main shock, and a brief description of the manifestation of a tsunami. A preliminary assessment of the macroseismic impact of the Kamchatka earthquake and its aftershocks revealed that the earthquake caused shaking of intensity 7–8 on the SIS-17 scale in Severo-Kurilsk and 6–7 in Petropavlovsk-Kamchatsky; no human casualties or serious damage caused by the earthquake and tsunami were recorded throughout the entire area of their propagation. Features of the source process development revealed by the results of the analysis of the diurnal variation of seismic energy released after the main event are discussed. The finite fault slip model of the earthquake based on the coseismic displacements from GNSS observations is presented.

Keywords: Kamchatka, strongest earthquakes, seismic focal zone, aftershocks, focal mechanism, macroseismics, tsunami, Kamchatka megathrust earthquake

Citation: Chebrov D. V., Matveenko E. A., Abubakirov I. R., Droznin D. V., Droznina S. Ya., Lander A. V., Mityushkina S. V., Pavlov V. M., Raevskaya A. A., Senyukov S. L., and Titkov N. N. (2026), The July 29, 2025 Kamchatka Earthquake, M_W 8.9: Examination Based on Regional Data Through End-2025, *Russian Journal of Earth Sciences*, 26, ES2006, EDN: EDEYBE, https://doi.org/10.2205/2026es001116

Research Article

Received: February 2, 2026
Accepted: May 25, 2026
Published: July 1, 2026

1. Introduction

On July 29, 2025, at 23:24 UTC, the strongest earthquake of planetary scale, $M_W = 8.9$[1], occurred near the Pacific coast of Kamchatka. It was named the "Kamchatka Earthquake". The earthquake became the sixth strongest seismic event in the world during the instrumental period (since the beginning of the 20th century) [*U.S. Geological Survey . . .*, 2026] and the strongest earthquake recorded by the regional seismic station network since the beginning of detailed seismological observations in Kamchatka and the Commander Islands in 1961 [*Gordeev et al.*, 2012].

[1] According to the KB GS RAS

The hypocenter of the Kamchatka earthquake was located at a depth of ≈44 km, approximately 146 km southeast of Petropavlovsk-Kamchatsky (http://sdis.emsd.ru/info/earthquakes/catalogue.php). According to the results of preliminary processing and assessment of macroseismic information, the Kamchatka earthquake was felt over most of the Kamchatka Peninsula, the Commander and Kuril Islands, with intensity[2] ranging from 2 to at least 7–8 at epicentral distances of 91–478 km. The maximum observed intensity of at least 7–8 was recorded in Severo-Kurilsk (Δ = 358 km). In Petropavlovsk-Kamchatsky (Δ = 146 km) and at the closest point[3] to the epicenter, at Cape Shipunsky (Δ = 91 km), shaking with an intensity of at least 6–7 was felt.

The Kamchatka earthquake generated a powerful tsunami [*Pinegina et al.*, 2026]; a warning was issued for most of the Pacific coast. In the area of Petropavlovsk-Kamchatsky, the water rise was insignificant; flooding of coastal lowlands and individual overwashes of sand spits and storm berms on the ocean shore were noted. Tsunami wave heights increased in the direction from north to south, and on the southern part of the eastern coast of Kamchatka reached over 15 m, but caused no damage due to the extremely sparse population of the territory and the location of the rare coastal structures (lighthouses and hydrometeorological stations) at considerable elevation. In Severo-Kurilsk, the population, upon the warning signal, managed to leave the town and move up into the hills; the arriving wave flooded the port and the fish processing plant buildings. Despite the proximity of the epicenter to populated areas and the exceptional strength of the earthquake, the Kamchatka earthquake and the associated tsunami caused no human casualties or serious destruction throughout the entire area of their manifestation.

The source of the Kamchatka earthquake was realized in the upper layer ($0 \le h \le 70$ km) of the Kamchatka seismic focal zone [*Chebrov et al.*, 2015; *Levina et al.*, 2013], whose seismic activity is among the highest in the world and is caused by the subduction process of the Pacific Plate beneath the Okhotsk Plate, on which Kamchatka and the Kuril Islands are located. The earthquake was preceded by a series of strong seismic events in the Avacha Gulf area, which began after a rather prolonged quiescence: the Vilyuchinsky earthquake of April 3, 2023 (M_W = 6.6) [*Chebrov et al.*, 2025b], the Shipunsky earthquake of August 17, 2024 (M_W = 7.0) [*Chebrov et al.*, 2025a], and finally, nine days before the main event, the Shipunsky-II earthquake of July 20, 2025 (M_W = 7.4).

According to data from [*Gusev and Shumilina*, 2004], GCMT[4], and the KB GS RAS (https://sdis.emsd.ru/map/?catalog=tensor&starttime=2010-01-01), the Kamchatka earthquake became the second strongest (in terms of moment magnitude M_W) event of the Kamchatka seismic focal zone recorded during the instrumental period, after the Great Kamchatka Earthquake of November 4, 1952 (M_W = 9.0) (Figure 1). It should be noted that there is exceptional similarity between the two strongest events in terms of epicenter locations (the distance between them is only 88 km), the sizes and configurations of their source areas, and the manifestations of the generated tsunami, which in the case of the Kamchatka earthquake did not have catastrophic consequences (Figures 1, 4). The absence of casualties from the tsunami generated by the Kamchatka earthquake is due not only to the favorable distribution of wave runups along the coast but also to the well-coordinated operation of all components of the Unified State System for the Prevention and Elimination of Emergency Situations, primarily the Tsunami Warning Service (TWS), for which operative information is provided by specialists of the Petropavlovsk Regional Data Processing Center (RDPC) KB GS RAS [*Chebrov*, 2007].

In accordance with the regulations of the Urgent Reporting Service (URS) GS RAS (http://www.gsras.ru) and the TWS, operative processing of the earthquake at the Petropavlovsk

[2] Here and hereafter, intensity I determined according to the SIS-17 scale (State Standard. GOST R 57546–2017 Earthquakes. Seismic Intensity Scale)

[3] Here and hereafter, the macroseismic points include populated areas, cordons (ranger stations), lighthouses, radionavigation and hydrometeorological stations (RNS and HMS), and others

[4] The Global Centroid Moment Tensor (GCMT) Project [*Dziewonski et al.*, 1981; *Ekström et al.*, 2012], http://www.globalcmt.org

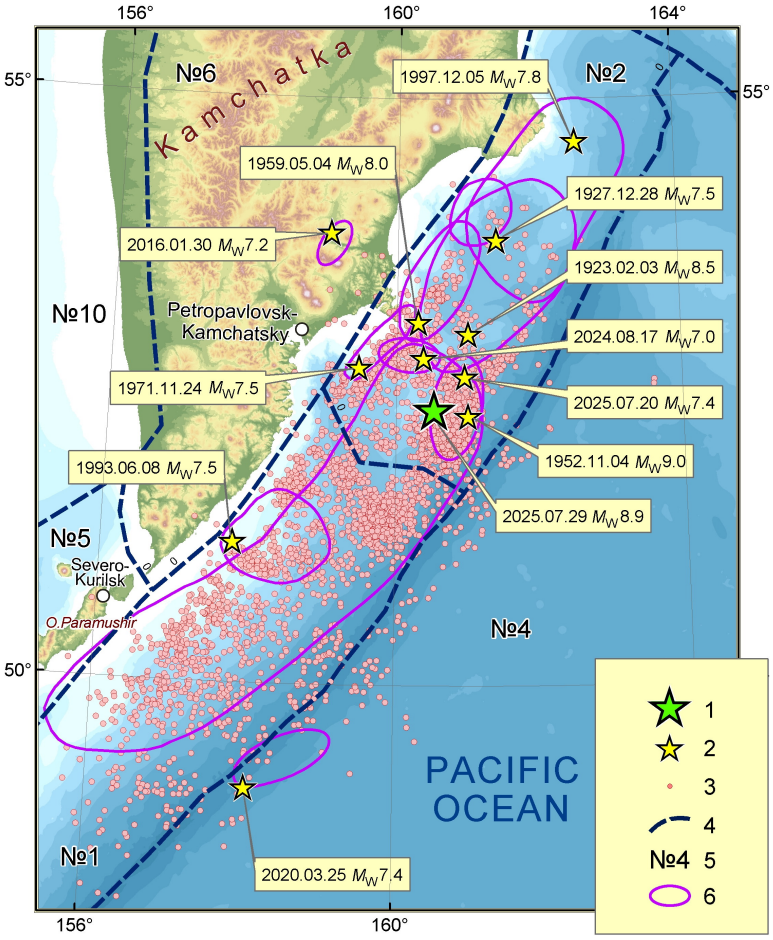

Figure 1. Epicenters and source areas of the Kamchatka earthquake and the strongest earthquakes in the Kamchatka seismic focal zone that preceded it in the depth range of 0–200 km, recorded since the beginning of instrumental observations worldwide according to [*Gusev*, 2004], GCMT and KB GS RAS catalogs in the moment magnitude scale M_W. 1 – epicenter of the Kamchatka earthquake; 2 – epicenters of the events that preceded the Kamchatka earthquake; 3 – aftershocks of the Kamchatka earthquake; 4 – boundaries of seismicity zones; 5 – seismicity zone number according to Lander [*Chebrov et al.*, 2015; *Levina et al.*, 2013]; 6 – contours of source zones.

RDPC began upon triggering of the alarm indicating that the seismic signal level had been exceeded at station RUS (Figure 3). Under conditions of very strong shaking lasting approximately four minutes, operators discovered that the dynamic range of the velocimeters, from whose recordings routine processing is conducted, had been exceeded, and that it was necessary to switch to accelerometers. Although some accelerometers ceased recording due to strong shaking and possible power interruptions, five minutes after the earthquake began, quick assessment of the source parameters were obtained from recordings of eight regional stations (Figures 2 and 3): origin time 23:24:49.5 UTC, φ = 52.4° N, λ = 160.5° E, h = 17 km, M_S = 7.0. According to data from the nearest strong motion station SPN (Δ = 90 km), the instrumental intensity automatically determined from strong motion station recordings of the KB GS RAS in near-real time [*Droznin et al.*, 2018] was 7; in Petropavlovsk-Kamchatsky, it ranged from 6 to 8; and in Severo-Kurilsk, it was 9. Based on the epicenter location in the Pacific Ocean and the tsunamigenic[5] magnitude M_S, a tsunami warning was issued, and telegrams were sent to the Tsunami Monitoring and Warning

[5] In accordance with the regulations of the Petropavlovsk RDPC, an earthquake with an offshore epicenter and $M_S \geq 7.0$ at the Petropavlovsk station (PET) is considered potentially tsunamigenic.

Center of the Kamchatka Department for Hydrometeorology and Environmental Monitoring, the Main Directorate of Emergency Control Ministry of the Russian Federation (EMERCOM) for Kamchatka Krai, the URS of the GS RAS, and warning services along the entire coast of Kamchatka and the Northern Kuril Islands. Processing and notification were completed within seven minutes after the earthquake began, which not only complies with the established regulations but also demonstrates the highest professionalism of the duty shift personnel.

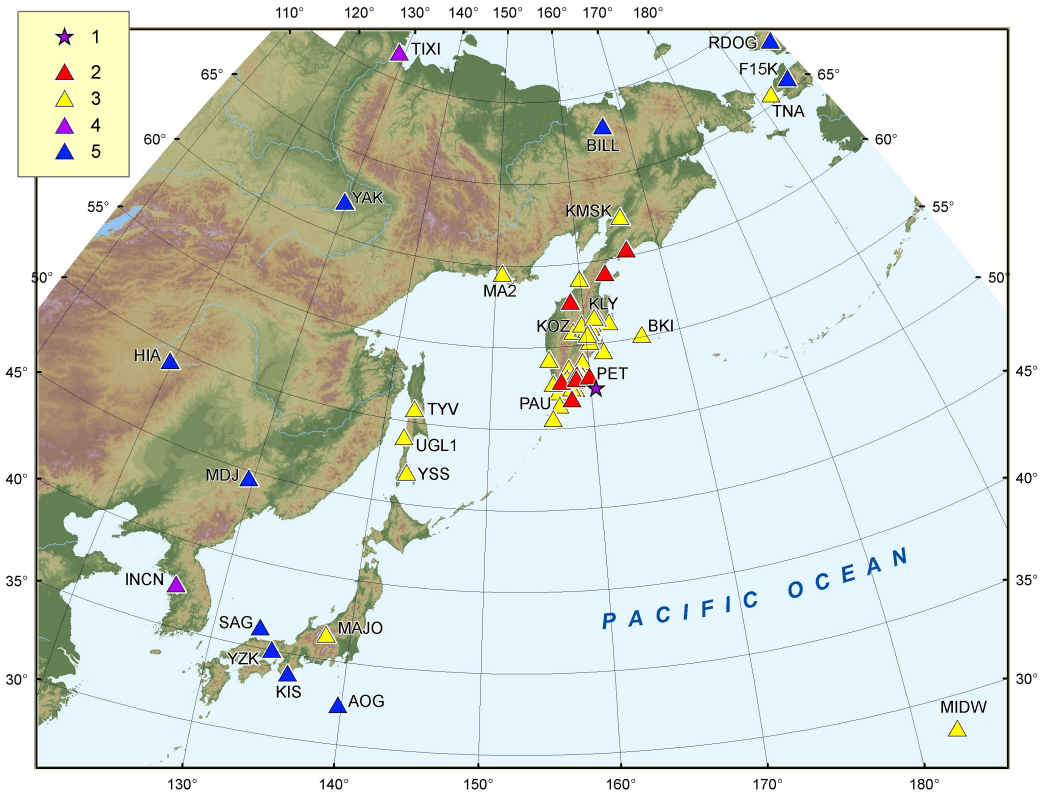

Figure 2. Stations involved in determining the parameters of the Kamchatka earthquake at the KB GS RAS. 1 – epicenter of the Kamchatka earthquake; 2 – stations involved both in quick processing according to the URS and TWS regulations, and in final processing; 3 – stations involved in final processing; 4 – stations involved both in final processing and in calculating the seismic moment tensor; 5 – stations involved in calculating the moment tensor.

In the first hours after the Kamchatka earthquake, its seismic moment tensor (SMT) was calculated at the KB GS RAS using the RSMT (Regional Seismic Moment Tensor) method from waveforms of broadband stations. From the parameters of tensor, the source mechanism and scalar seismic moment were determined, which made it possible to estimate the moment magnitude $M_W = 8.9$. Within the RSMT method, simultaneously with the calculation of the SMT, an estimate of the rupture duration $\tau = 224$ s was obtained. The rupture began in the northern part of the source at the latitude of Avacha Gulf and propagated in a southwest direction toward Paramushir Island over a distance of approximately 580 km.

Final processing of the Kamchatka earthquake was performed within the first 24 hours using data from 69 stations located on the Kamchatka Peninsula, the Russian Far East, and territories of neighboring countries (Figures 2 and 3) [*Senyukov et al.*, 2025]. The results of the regional observation system are in good agreement with data from global agencies (Table 1).

Table 1. Coordinates of the hypocenter and magnitudes of the Kamchatka earthquake according to data from various seismological agencies

No.	Agency	Time, hh:mm:ss	$\varphi°$, N	$\lambda°$, E	h, km	Magnitude / Number of stations
1	KAGSR[1]	23:24:49.83	52.36	160.53	43.7	M_W=8.9/12, M_L^2=7.5, M_c^3=8.4/17
2	GSRAS	23:24:50.00	52.43	160.46	20.0	M_S=8.2, m_b=7.1
3	NEIC[4]	23:24:52.48	52.50	160.24	35.0	m_b=7.0/1147, M_{s_20}=8.0/629, M_{WW} = 8.8/303
4	GCMT (centroid)	23:26:49.70	50.36	158.23	36.3	M_W=8.7/170
5	GFZ[5]	23:24:52.78	52.52	160.12	27.1	M_W=8.8

[1] KB GS RAS, https://emsd.ru/
[2] Local magnitude $M_L = 0.5 \cdot K_S - 0.75$ [*Chubarova et al.*, 2010], where K_S is the energy class [*Fedotov*, 1972]
[3] Magnitude Mc from coda waves [*Gordeev et al.*, 1999]
[4] National Earthquake Information Center, https://www.usgs.gov/staff-profiles/national-earthquake-information-center-neic
[5] GFZ German Research Centre For Geosciences, http://www.gfz-potsdam.de

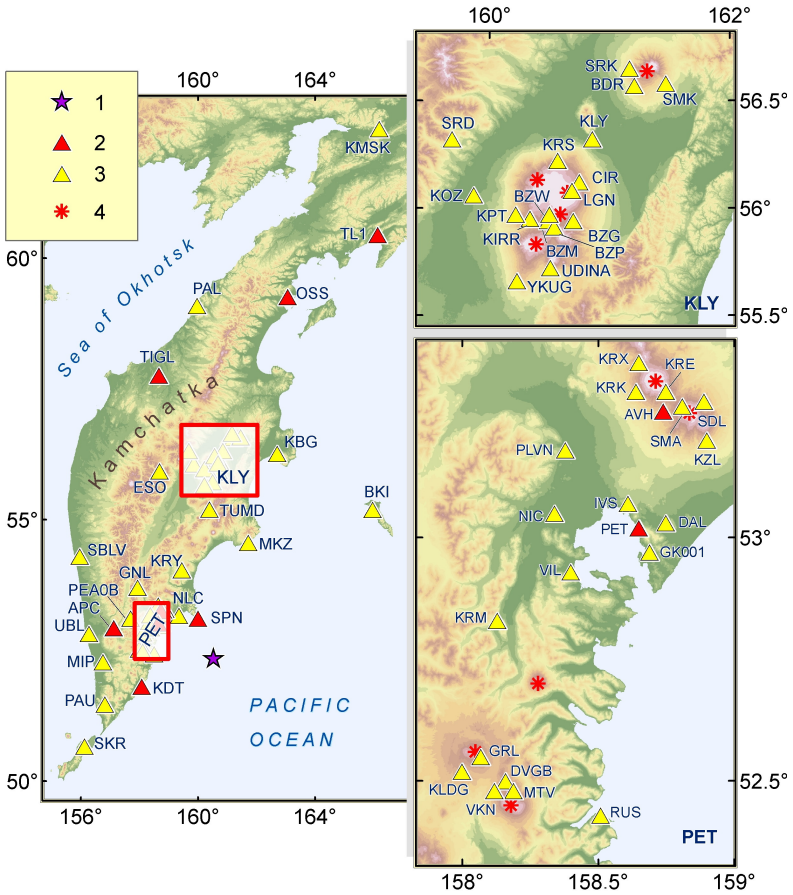

Figure 3. Stations of the Kamchatka seismic network and SKR station of the Sakhalin Branch of the GS RAS, involved in the rapid and definitive processing of the main parameters of the Kamchatka earthquake at KB GS RAS. 1 – epicenter of the Kamchatka earthquake; 2 – stations used for both rapid processing (according to the URS and TWS regulations) and final processing; 3 – stations used for final processing only; 4 – volcanoes.

2. Aftershock Process of the Kamchatka Earthquake and Features of Event Processing in the Source Region

For the rapid assessment of the aftershock process development under conditions of high earthquake density, a standard automatic single-station detection procedure, developed at the KB GS RAS [*Chebrov et al.*, 2021] and integrated into the DIMAS earthquake processing software [*Droznin and Droznina*, 2011], was applied. As a result of the detector's operation, a station bulletin is created, containing the time and energy estimate of all events recorded by the selected station, and a request for data selection for processing is generated. For the period from July 29 to December 31, 2025, based on data from station RUS, one of the closest stations to the epicenter of the Kamchatka earthquake, the detector identified approximately 30,000 events from the epicentral zone. At the time of writing, 3,801 aftershocks in the source region, with M_L = 1.7–7.2 occurring in the above period, have been located: the parameters of earthquakes with $M_L \geq 5.3$ (475 events) have been calculated without gaps, as well as for the majority of events with $M_L \geq 4.3$. Processing of the remaining earthquakes for July 29 – December 31, 2025 is ongoing in 2026 in parallel with the current processing of continuing aftershocks. The completeness of the resulting catalog, including the main event, at the time of writing is estimated as $M_L^C = 5.6$ with a statistical significance of $\alpha = 0.3$ [*Saltykov*, 2019], which is significantly higher than the completeness magnitude of the Kamchatka earthquake catalog ($M_L^C = 3.5$), and is still insufficient for a detailed assessment of the process.

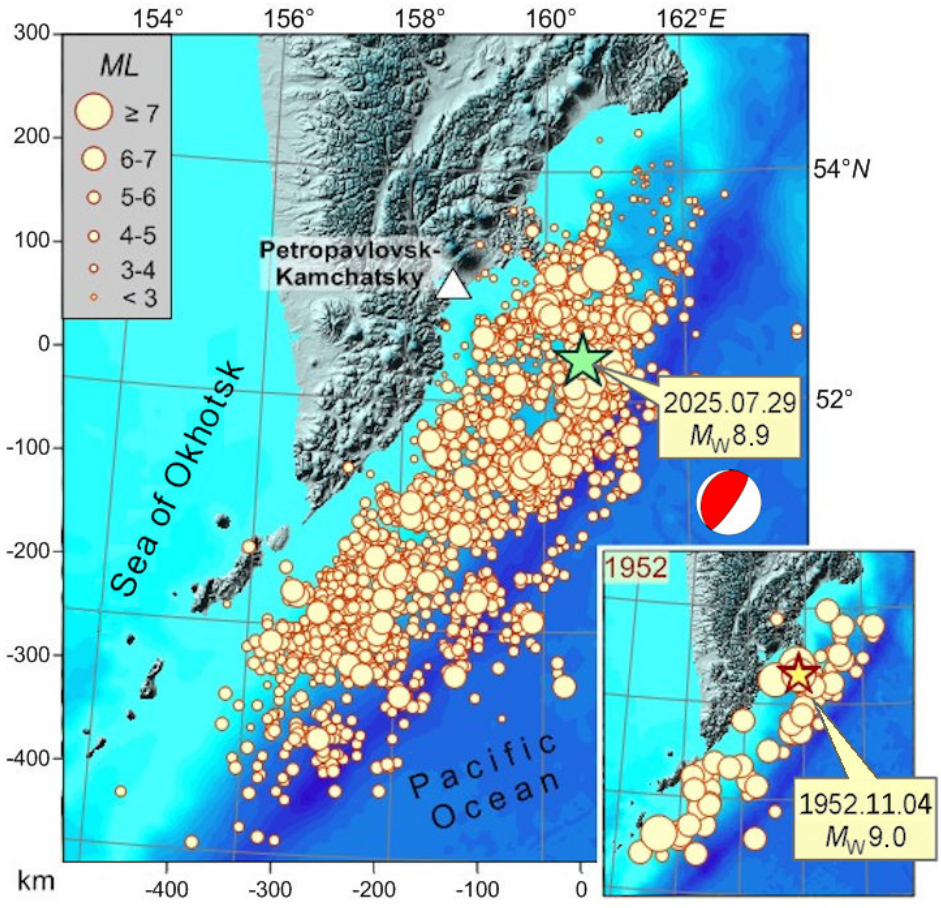

Figure 4. Epicenters of the Kamchatka earthquake and its aftershocks according to the Kamchatka regional catalog for the period from the mainshock to December 31, 2025, inclusive. Inset: the November 4, 1952, M_W 9.0 earthquake with aftershock epicenters for the same time period (5 months). Stars are the epicenters of the main events according to the ISC catalog (https://www.isc.ac.uk/iscbulletin/search/catalogue/).

Six events of the aftershock sequence of the Kamchatka earthquake had magnitude $M_L \geq 6.5$ ($M_W \geq 6.1$). The two strongest among them ($M_W \geq 7.0$) were recorded near Cape Shipunsky on September 13 at 02:37 UTC with $M_W = 7.4$ and on September 18 at 18:58 UTC with $M_W = 7.8$. Their hypocenters were located at depths of approximately 46 and 48 km, approximately 122 and 143 km east of Petropavlovsk-Kamchatsky, respectively. According to data from the nearest strong motion station SPN ($\Delta = 32$ and 51 km), the instrumental intensity of shaking caused by these events was 7.3 and 7.9. The maximum observed shaking intensity $I = 6$ for both earthquakes was recorded at Cape Shipunsky, while in Petropavlovsk-Kamchatsky ($\Delta = 122$ and 143 km) it reached 5 and 5–6, respectively. The main event exceeded the strongest aftershock by $\Delta M_W = 1.1$, which is consistent with Båth's law [*Båth*, 1965]. The source size, estimated from the aftershock cloud, is 580 × 180 km.

Let us consider the obtained aftershock catalog from the perspective of its consistency with current understanding of the position of the Kamchatka earthquake source in the upper layer of the Kamchatka seismic focal zone. Hypocenter parameters were calculated using the DIMAS program by iterating over depth and origin time. For each variant, the geographical coordinates of the event are determined; the solution with the minimum root-mean-square value of travel-time residuals is taken as final. The velocity model from [*Melnikov*, 1990] is used in the calculations. In Figures 5(*b*, *c*), attention is drawn to clusters of hypocenters of the Kamchatka earthquake aftershocks beneath the boundaries of the layers at depths of 20 and 40 km, which may be related to a complex of methodological factors related to the accuracy of the travel-time curve used, the picking of arrivals, and the configuration of the station network. The obtained hypocenter distribution apparently does not reflect the real situation, which should be kept in mind when attempting to interpret these data.

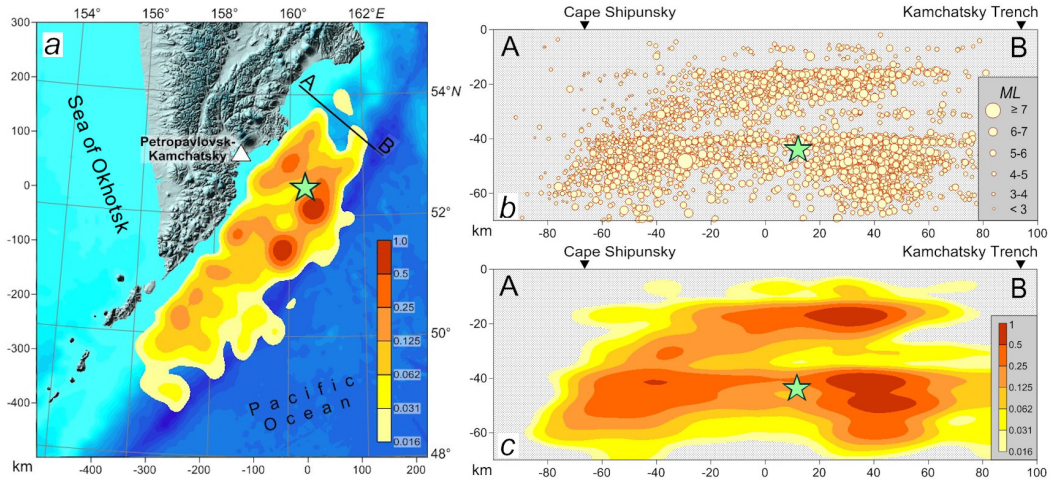

Figure 5. (*a*) Smoothed relative density of aftershock epicenters (ignoring magnitude) from the Kamchatka and Commander Islands Earthquake Catalog. The density map is normalized to its maximum. Line AB is the trace of the vertical plane onto which the hypocenters were projected when constructing the cross-sections in the figures on the right. (*b*) Projection of the complete aftershock cloud onto vertical plane AB in the figure on the left, orthogonal to the strike of the Kamchatka Trench. (*c*) Smoothed relative density of aftershock hypocenter projections onto plane AB (ignoring magnitude). The density map is normalized to its maximum. The star is the epicenter of the Kamchatka earthquake.

A different picture is observed in Figure 6(*b*, *c*) for the alternative version of the aftershock catalog, calculated using the HMM program, which is based on the minimax criterion for hypocenter location [*Lander et al.*, 2019]. The same seismic phase arrival times that were used in creating the Kamchatka Regional Catalog were utilized. However, the velocity model was changed – a simplified homogeneous single-layer model of the continental crust with a thickness of 40 km, a P-wave velocity of 6 km/s, and a fixed V_p/V_s

ratio of 1.73 was used. As a result, it was possible to obtain an aftershock cloud that clearly delineates the upper shallow-dipping segment of the subduction zone.

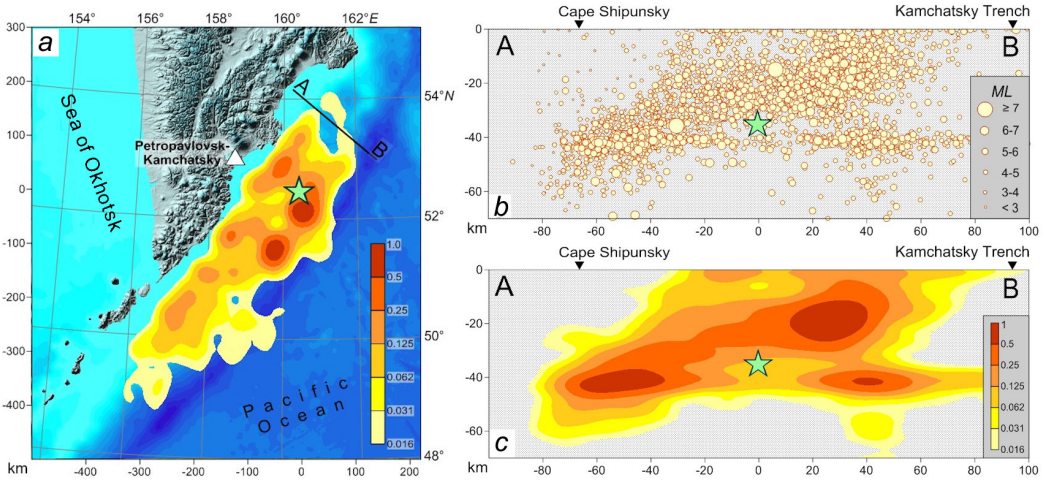

Figure 6. (*a*) Smoothed relative density of aftershock epicenters (ignoring magnitude), calculated using the HMM program. The density map is normalized to the maximum. Line AB is the trace of the vertical plane onto which the hypocenters were projected when constructing the cross-sections in the figures on the right. (*b*) Projection of the complete aftershock cloud onto vertical plane AB in the figure on the left, orthogonal to the strike of the Kamchatka Trench. (*c*) Smoothed relative density of aftershock hypocenter projections onto plane AB (ignoring magnitude). The density map is normalized to the maximum. The star is the epicenter of the Kamchatka earthquake.

2.1. Features of the Development of the Source Process of the Kamchatka Earthquake Based on Data Obtained by December 31, 2025

Since the aftershock process of the Kamchatka earthquake has not yet ended and complete data processing has not been performed, a detailed analysis of its development is difficult both in terms of the aftershock flow intensity [*Utsu*, 1970] and energy release [*Gospodinov and Rotondi*, 2006; *Ogata*, 1988]. However, even from the existing limited dataset, a number of features can be identified as a basis for assumptions about the further development of the aftershock process. For this purpose, we will examine the course of released seismic energy. This approach is preferable in the given conditions than analyzing the aftershock flow intensity, since it is less sensitive to the completeness of the catalog in the low-magnitude range.

We will consider the total energy released per calendar day, using the well-known relationship: $\lg E[\mathrm{J}] = 1.5M + 4.8$ [*Gutenberg*, 1956], substituting the moment magnitude M_W according to the definition [*Kanamori*, 1977]. Priority is given to the moment magnitude from the Kamchatka Regional Catalog, calculated using the RSMT method; when such determinations are absent, magnitudes from the NEIC and GCMT catalogs are used; for weak events, a conversion from local magnitude M_L is performed using the relationship from [*Abubakirov et al.*, 2018]. The value of the daily total released energy will be plotted on the left axis (Figure 7), with day numbering starting from zero (the day of the main shock); the value for day zero is not plotted. On the right axis, we will plot the released energy on a logarithmic scale, using the inverse relationship $M_W = \frac{2}{3}\lg\sum_i E_i - 3.2$, where the sum of energies of aftershocks occurring during the day is under the decimal logarithm. In meaning, this corresponds to a situation where all energy released during the current day was realized in a single event; therefore, we will here call this quantity the equivalent magnitude.

Let us highlight the characteristic features of the source process.

1. Two stages of its development can be identified, which are separated by the strongest aftershocks of September 13 and 18 with M_W = 7.4 and 7.8. The energy release

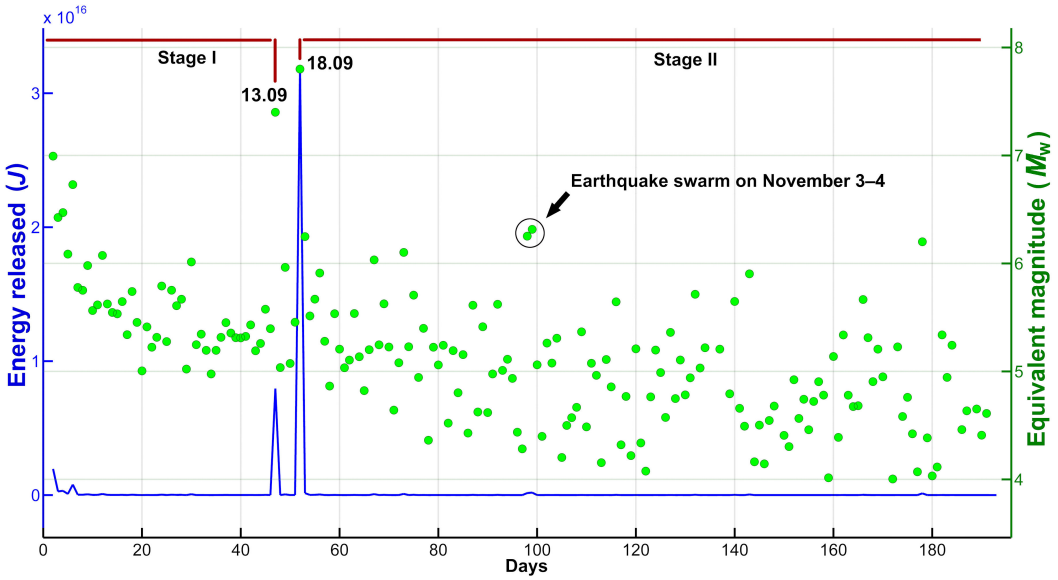

Figure 7. Daily course of energy release during the aftershock process of the Kamchatka earthquake from the first day after the main event to December 31, 2025 inclusive.

regimes at these stages differ significantly. It should be noted that a change in regime after the strongest aftershocks has frequently been observed in global practice, including for Kamchatka earthquakes [*Saltykov*, 2025].

2. For the first stage, a power-law decay of the released energy can be assumed. In this case, the variance of the values (on a log-linear scale – on the right axis of Figure 7) is relatively small. Thus, fairly quickly (within 12 days), the energy release drops to moderate values and remains in the range of $5 < M_W < 6$, i.e., both "quiet" days (with $M_W < 5$) and "intense" days are completely "forbidden." This continues until the pair of strongest aftershocks.
3. In the second stage, a sharp increase in variance is observed, and overall a tendency toward a decrease in daily energy release is evident. As a result, "quiet" days become "allowed" (down to equivalent magnitude values of $M_W = 4$). At the same time, "intense" days with equivalent magnitude $M_W > 6.0$ are possible, but their frequency is expectedly decreasing. It can be assumed that after 200 days of the aftershock process, the probability of a strong aftershock with $M_W > 6.0$ will be negligible.
4. Also for the second stage, an uneven and pulsating character of energy release can be noted, which becomes particularly noticeable after day 120.

Additionally, let us note an interesting event, which in Figure 7 is highlighted by two relatively high equivalent magnitude values on days 98 and 99 of the aftershock process (November 3 and 4, 2025). On these days, the swarm activation was observed, which occurred in the Pacific Ocean opposite Avacha Gulf. The total energy of this swarm corresponds to a magnitude of $M_W = 6.4$; thus, it can be considered the strongest event during the relaxation process of the source zone.

2.2. Mechanism and Source Parameters of the Kamchatka Earthquake

At the KB GS RAS, seismic moment tensors (SMT) of regional earthquakes are determined using the RSMT method [*Abubakirov and Pavlov*, 2021; *Pavlov and Abubakirov*, 2012] by fitting three-component waveforms recorded by seismic stations in the regional range of epicentral distances, using complete synthetic seismograms calculated for a layered half-space. Real and synthetic waveforms, including body and surface waves, are filtered in a period band that depends on the magnitude, epicentral distance, and type of recording equipment. Simultaneously with the SMT, the duration τ of the source time function and the depth h_e of the equivalent point source (EPS) are estimated. For the SMT inversion the

latitude and longitude of the EPS are input parameters, which for relatively small events are fixed at the epicenter coordinates and for large events could be tied to the centroid position from external agencies (GCMT, NEIC etc.). Estimates of source parameters are determined for two types of tensors: DC (Double-Couple) – a double-couple without torque (nonlinear inversion), and NT (Null Trace) – a zero-trace tensor (linear inversion). From the SMT, the source mechanism and the scalar seismic moment M_0 are determined. The moment magnitude M_W is recalculated from M_0 using the formula $M_W = 2/3(\lg(M_0[\mathrm{N}\cdot\mathrm{m}]) - 9.1)$ [*Kanamori*, 1977].

Estimates of the source parameters of the Kamchatka earthquake of July 29, 2025 were obtained from waveforms of 12 broadband seismic stations from the Russian Far East, Alaska, and Japan, located at epicentral distances ranging from 2,000 to 3,000 km (Figure 2). The waveforms were filtered in the period band of 200–500 s. The latitude and longitude of the centroid were specified according to the GCMT catalog. Table 2 presents the estimates of the source parameters of the Kamchatka earthquake obtained at the KB GS RAS for DC-type and NT-type tensors, as well as NT solutions from the GCMT, NEIC, and GFZ catalogs, calculated from waveforms of global network seismic stations. The NT solutions contain Lode–Nadai parameter values [*Yunga*, 1979] ranging from –13% to 3%. This means that the non-DC component of the seismic moment tensor is negligibly small, and the obtained solutions correspond to the DC model. To describe the mechanism in the NT models, the parameters of the best (closest) double couple were used [*Ekström et al.*, 2012]. The focal mechanisms in all solutions were close to each other (the maximum Kagan angle [*Kagan*, 2007] between the triplets of principal axes is 26°). Estimates of the moment magnitude M_W ranged from 8.7 to 8.9; centroid depth values are in the range of 21–36 km. Estimates of the source process duration τ obtained at the KB GS RAS (224 s) and at the USGS NEIC (225 s) by direct calculation coincide to within one second, and are almost twice the τ value from the GCMT catalog (113.4 s), which was obtained using a empirical relationship.

2.3. Operative Determination of Mechanisms and Source Parameters of the Kamchatka Earthquake Aftershocks

As of December 31, 2025, the Catalog of Earthquakes of Kamchatka and the Commander Islands contained 794 earthquakes with $M_L \geq 5.0$ that occurred in the source region of the Kamchatka earthquake after the main event. Due to the impossibility of promptly determining focal mechanisms and parameters using the RSMT method for all aftershocks with $M_L \geq 5.0$, the threshold for priority processing was raised to $M_L \geq 6.0$, and then weaker events were processed as feasible. By December 31, 2025, a total of 120 earthquakes with $M_L = 5.6$–7.2 from the aftershock sequence had been processed in an operative mode using the RSMT method. Of these, mechanisms and source parameters were determined for 97 earthquakes with $M_W = 4.7$–7.8 (Figure 8, section A); for 23 of them, it was not possible to determine the mechanisms and source parameters due to insufficient data with an acceptable signal-to-noise ratio. The maximum moment magnitude values of $M_W \geq 7.0$ were obtained for the two strongest aftershocks – September 13 ($M_W = 7.4$) and September 18 ($M_W = 7.8$).

Table 2. Summary of parameters of the Kamchatka earthquake source

No.	Agency, method	Principal axes and Principal values (in units 10^{22} N·m)									Mechanism						M_W	M_0 10^{22} N·m	h, km	τ, s	η, %	Tensor diagram
		T			N			P			NP1		D1		NP2		D2						
		E_T	pl°	azm°	E_N	pl°	azm°	E_P	pl°	azm°	stk°	dip°	slip°	stk°	dip°	slip°						
1	KAGSR, RSMT-DC	2.91	61	309	−0.00	3	213	−2.91	29	122	203	16	79	34	74	93	8.91	2.91	25.0[1]	224.0[2]	0	
2	KAGSR, RSMT-NT	2.86	61	304	0.06	2	211	−2.92	29	120	206	16	84	32	74	92	8.91	2.89	25.0[1]	224.0[2]	3	
3	GCMT	1.58	63	313	−0.01	2	219	−1.57	27	128	214	18	84	40	72	92	8.73	1.58	36.3[3]	113.4[4]	−1	
4	NEIC-WP	2.31	58	344	−0.19	11	236	−2.12	30	139	198	18	51	58	76	101	8.83	2.22	21.5[3]	225.0[2]	−13	
5	GFZ	1.95	57	321	−0.08	3	225	−1.87	32	133	209	13	73	46	77	93	8.79	1.91	21.0[5]	–	−6	

[1] depth of the equivalent point source;
[2] calculation result;
[3] centroid depth;
[4] assessment based on empirical relationship from [*Ekström et al.*, 2012];
[5] depth of the hypocenter.

Note: DC – double-couple tensor without moment; NT – null-trace tensor; E_T, E_N, E_P – principal eigenvalues of the tensor; h – source depth; τ – duration; η – Lode–Nadai parameter: $\eta = (2E_N - E_T - E_P)/(E_T - E_P) \times 100\%$. WP – W-phase; CMT – Centroid Moment Tensor; M_W – moment magnitude; M_0 – scalar seismic moment (for RSMT-NT, GCMT, and GFZ solutions, M_0 is calculated using the formula $M_0 = (E_T - E_P)/2$; for NEIC solution, $M_0 = \sqrt{(E_T^2 + E_N^2 + E_P^2)/2}$); pl, azm – angles defining the orientation of the T, N, P principal axes; stk, dip, slip – angles defining the orientation of the nodal planes. The right column shows the corresponding seismic moment tensor diagrams in equal-area projection of the lower hemisphere.

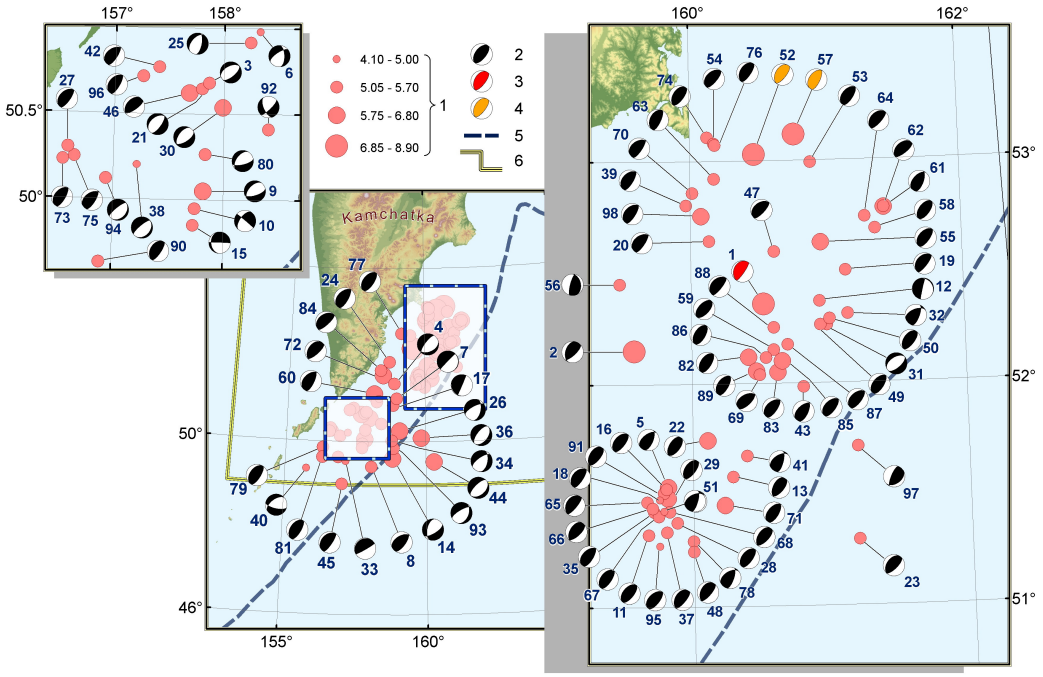

Figure 8. Source mechanisms of the Kamchatka earthquake and its aftershocks determined as of December 31, 2025. 1 – earthquake epicenter in the corresponding range of moment magnitude M_W; 2 – stereogram of the earthquake source mechanism in the equal-area projection of the lower hemisphere of the focal sphere; 3 – mechanism of the main event; 4 – mechanisms of the strongest aftershocks of September 13, M_W = 7.4 and September 18, M_W = 7.8; 5 – deep-sea trench; 6 – boundaries of the responsibility area of the KB GS RAS.

The obtained RSMT estimates are in good agreement with global determinations. For 73 events from the RSMT catalog that have solutions in the GCMT catalog, a comparison was performed of the M_W, h_e, and focal mechanism estimates (Figure 9).

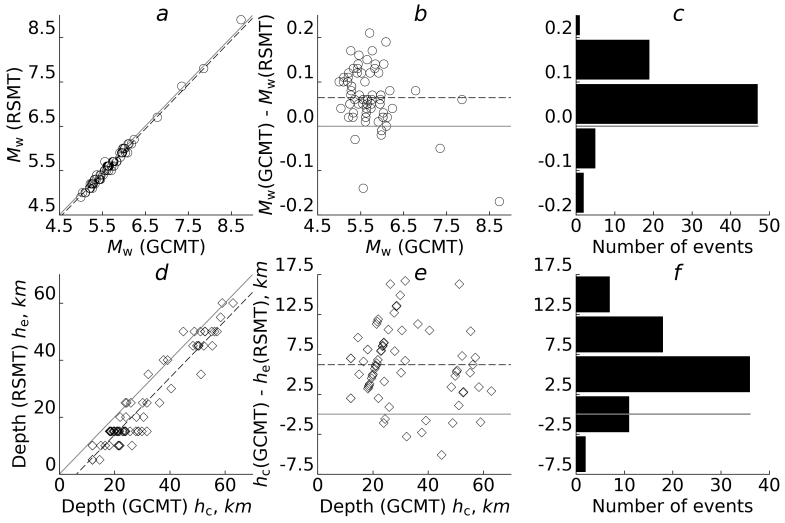

Figure 9. Comparison of the estimates of the moment magnitude M_W (*a*)–(*c*) and the depth h_e of the equivalent point source (*d*)–(*f*), presented in Table 2, with the solutions from the GCMT catalogue. The solid line in (*a*, *d*) marks the points for which the corresponding estimates coincide; in (*b*, *e*) the differences are plotted; the dashed line in (*a*, *b*, *d*, *e*) denotes the mean values: 0.06 for ΔM_W and 6.2 km for Δh, the standard deviations are 0.06 and 4.6 km. In (*c*, *f*) the histograms of the dependence for (*b*, *e*), respectively, are shown.

The maximum absolute value of the difference $\Delta M_W = M_W$ (GCMT) – M_W (RSMT) is 0.21 magnitude units, and for 91% of events it does not exceed 0.1. The mean value $\mu(\Delta M_W) = 0.06$; the standard deviation $\sigma(\Delta M_W) = 0.06$. The maximum absolute value of the difference $\Delta h = h_c$(GCMT) – h_e(RSMT) reaches 17 km, and for 69% of events it does not exceed 10 km. The mean value $\mu(\Delta h) = 6.2$ km, the standard deviation $\sigma(\Delta h) = 4.6$ km. The Kagan angle K [*Kagan*, 2007] between the triplets of principal axes of the RSMT focal mechanisms (DC) and the best double couples (BDC) of GCMT for all events lies in the range of 0–25° (Figure 10).

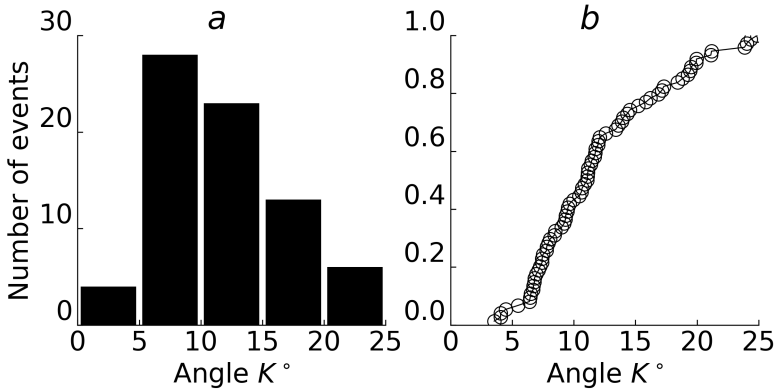

Figure 10. Histogram (*a*) and empirical cumulative distribution function (*b*) of the values of the angle K between the triples of the principal axes of the RSMT (DC) and GCMT (BDC) mechanisms.

Classification of focal mechanisms according to the types of slip in the source (Table 3) was performed based on the plunge angles of the principal axes [*Volfman et al.*, 2022]. The majority (74%) of the aftershocks, like the main event, are reverse events, 18% are normal faults, and 8% are normal-strike-slip, strike-slip-normal, and strike-slip-thrust events.

The mechanisms of aftershocks with a thrust-type slip are close to the mechanism of the main event (Figure 11). The angle K between the triplets of principal axes of the main shock and the aftershocks of this group does not exceed 32° in 70 cases out of 72. The value of angle K ranges from 7° to 61° (with a maximum possible value of 120°); the mean value $\mu(K) = 20°$, and the standard deviation $\sigma(K) = 8°$.

Table 3. Distribution of mechanisms of aftershocks of the Kamchatka earthquake for the period July 29 – December 31, 2025 according to the types of movement in the source based on classification according to the plunge angles of the main axes

Type of mechanism	The range of values of the plunge angles P_{pl}, N_{pl}, T_{pl} of the principal axes P, N and T			Number of earthquakes
	P_{pl}	N_{pl}	T_{pl}	
Reverse	≤30°	≤30°	≥45°	72
Normal	≥45°	≤30°	≤30°	17
Strike-slip	≤30°	≥45°	≤30°	0
Thrust-Strike-slip	≤30°	>30°	>30°	0
Normal-Strike-slip	>30°	>30°	≤30°	3
Strike-slip-Normal	>45°	<30°	30° < T_{pl} ≤45°	2
Strike-slip-Thrust	30° < P_{pl} ≤45°	<30°	>45°	3
Total				97

2.4. Source Model of the Kamchatka Earthquake Based on Global Navigation Satellite System (GNSS) Data

The Kamchatka earthquake caused significant coseismic displacements of the Earth's surface on the Kamchatka Peninsula, the western coast of the Sea of Okhotsk, the Kuril

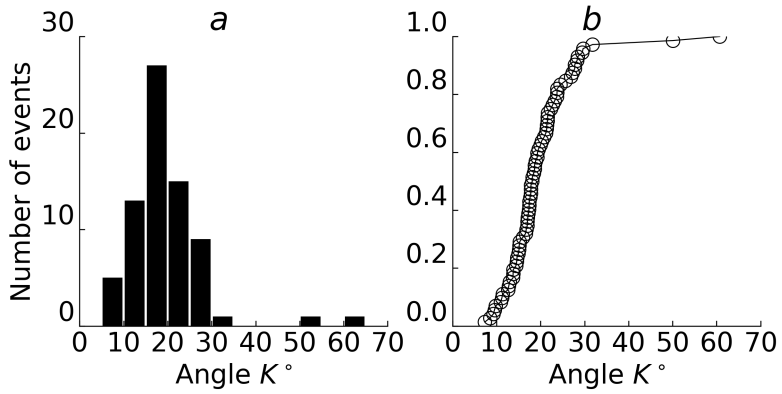

Figure 11. Comparison of source mechanisms for the Kamchatka earthquake of July 29, 2025, and its aftershocks with reverse-fault slip for the period from July 29 to December 31, 2025, obtained at the KB GS RAS using the RSMT method. *a* – histogram of the Kagan angle (K) values between the triplets of the principal axes of the mainshock and aftershock mechanisms (mean value μ=20° and standard deviation σ=8°); *b* – empirical cumulative distribution function of the K angle.

Islands, and Sakhalin Island (Table 4). The largest horizontal displacements, reaching up to 2 m, were recorded in the south of the Kamchatka Peninsula and on Paramushir Island, in the area of maximum slip along the fault surface. GNSS data processing at the KB GS RAS was performed using the GAMIT/GLOBK software package, version 10.71. Data from the regional GNSS network were processed together with data from ten IGS stations (AIRA, BJFS, GOLD, GUAM, KOKB, MAUI, SHAO, SUWN, WHIT, WUHN), which were taken as reference stations. Subsequently, a secondary adjustment was performed within the IGS network, using approximately 190 IGS stations as references; covariance matrices from the IGS network based on SOPAC combined solutions were used in the calculations. Time series of daily coordinates were generated, and coseismic displacements were determined as the distance between regression lines at the time of the earthquake.

A portion of the measured coseismic displacements presented in Table 4 was used to construct a source model of the Kamchatka earthquake (Figure 12). Ten GNSS stations, closest to the source and having the smallest relative errors, were selected. Both horizontal and vertical components of the displacements were used.

The model consists of a set of polygons of initially unknown arbitrary shape lying in a single plane (strike 220°, dip 28°). Within each polygon, the slip is assumed to be unknown but uniform. A polygon of arbitrary shape is composed of point sources, whose effect on the ground surface is calculated using Okada's formulas [*Okada*, 1985]. For each specified intermediate or final source model, the fields of surface horizontal and vertical displacements are calculated over a specified area and, in particular, the modeled movements of selected GNSS stations, which are compared with measurements. The calculation is implemented in the program OKAPOLIA, written by A. V. Lander. The initial shape of the polygons comprising the source model was chosen based on the distribution of aftershocks during the first week after the main event. Empirical relationships between source slip and magnitude and rupture area were used when selecting the initial slip values. Subsequently, a sequential adjustment of the source polygon shapes and slip values was performed to achieve a better fit with the GNSS data. The best fit between the model and the data was obtained for an earthquake with a magnitude of M_W = 8.7. According to the resulting source model, its dimensions reached approximately 520 × 160 km, and the maximum source slip reached 14 m.

2.5. Brief Overview of the Macroseismic Effect of the Kamchatka Earthquake

The primary tool for collecting, assessing, and analyzing information on macroseismic manifestations of regional earthquakes at the KB GS RAS is an interactive questionnaire

Table 4. Coseismic displacements caused by the Kamchatka earthquake

No.	Station	$\varphi°$, N	$\lambda°$, E	East, mm	North, mm	Up, mm
1	APC1	−52.926	157.133	396.7 ± 5.5	−426.8 ± 6.8	−16.5 ± 5.9
2	ARSN	53.066	158.589	357.5 ± 4.4	−526.8 ± 7.9	−64.3 ± 4.8
3	ATLS	55.606	159.648	10.2 ± 2.1	−35.4 ± 2.8	−11.2 ± 6.8
4	AVCH	53.264	158.740	241.4 ± 3.3	−412.5 ± 7.0	−46.6 ± 4.6
5	AYN1	56.466	138.176	15.7 ± 1.5	−7.5 ± 2.5	−4.0 ± 7.2
6	BRNG	55.194	165.984	−0.6 ± 2.2	1.5 ± 2.4	−7.2 ± 8.5
7	BZ07	55.952	160.343	4.7 ± 1.5	−21.8 ± 1.8	1.5 ± 5.0
8	BZGD	55.940	160.696	4.6 ± 2.0	−17.5 ± 3.1	−3.1 ± 7.0
9	CIR1	56.117	160.748	3.7 ± 1.9	−14.7 ± 2.4	8.4 ± 5.8
10	_ES1	55.930	158.697	14.3 ± 1.5	−46.0 ± 2.1	0.2 ± 6.9
11	ITRP	45.254	147.887	5.0 ± 1.1	−0.8 ± 1.8	1.9 ± 9.5
12	_KBG	56.258	162.711	2.6 ± 2.2	−2.4 ± 2.0	16.7 ± 17.9
13	KLCH	56.318	160.856	3.6 ± 3.4	−14.7 ± 2.8	−2.0 ± 11.2
14	KLU1	56.318	160.856	3.3 ± 4.2	−15.2 ± 2.5	7.4 ± 6.4
15	KMS1	62.467	166.206	0.3 ± 2.9	−3.8 ± 2.8	−0.5 ± 5.4
16	KMSH	52.827	158.131	488.9 ± 5.1	−597.2 ± 8.4	−86.7 ± 6.7
17	KOZS	56.057	159.873	6.2 ± 1.8	−25.7 ± 2.8	−6.8 ± 6.8
18	KRC1	53.283	158.212	272.5 ± 4.1	−411.9 ± 7.3	−28.3 ± 4.1
19	KZLS	53.202	158.899	287.7 ± 7.0	−434.1 ± 22.9	−44.7 ± 66.9
20	MAG1	59.577	150.810	13.0 ± 1.6	−19.2 ± 1.9	4.1 ± 5.4
21	MIL4	54.695	158.621	38.9 ± 2.0	−102.2 ± 2.8	1.6 ± 8.3
22	MYAK	52.889	158.707	474.0 ± 6.0	−610.7 ± 9.8	−103.5 ± 9.2
23	NGL2	51.812	143.155	32.1 ± 1.8	−4.7 ± 1.5	−5.3 ± 7.2
24	OLM3	59.574	151.294	14.9 ± 2.0	−22.0 ± 2.1	5.3 ± 5.9
25	OSSS	59.262	163.072	2.1 ± 3.4	−5.0 ± 2.4	11.0 ± 10.9
26	OXTK	59.360	143.235	15.9 ± 1.4	−12.8 ± 2.1	1.2 ± 6.5
27	PARM	50.670	156.116	1461.3 ± 9.2	−851.7 ± 7.1	−186.1 ± 17.7
28	PAUJ	51.469	156.815	1312.4 ± 10.0	−927.8 ± 7.7	−230.7 ± 13.2
29	PETR	53.067	158.607	355.7 ± 4.2	−527.5 ± 8.1	−68.1 ± 6.9
30	PETS	53.023	158.650	382.6 ± 4.9	−546.9 ± 7.8	−76.7 ± 15.2
31	PETT	53.080	158.640	347.5 ± 4.5	−521.7 ± 7.9	−65.7 ± 3.8
32	PGDN	56.263	162.585	1.5 ± 1.5	0.3 ± 1.8	3.7 ± 5.9
33	PPK1	53.081	158.640	347.7 ± 4.7	−520.4 ± 7.8	−66.1 ± 8.8
34	PRVM	49.960	143.269	25.6 ± 2.8	4.2 ± 3.1	8.6 ± 7.0
35	RADZ	53.074	158.986	330.8 ± 4.5	−504.8 ± 6.8	−87.0 ± 5.2
36	SKR3	50.668	156.114	1467.2 ± 10.2	−859.2 ± 8.1	−182.5 ± 15.8
37	SPNS	53.106	160.011	123.7 ± 4.9	−218.9 ± 5.0	−71.7 ± 8.7
38	TIGS	57.765	158.671	5.8 ± 1.8	−20.5 ± 1.5	−0.7 ± 4.6
39	UBR3	52.824	156.281	382.0 ± 5.0	−362.8 ± 6.3	7.0 ± 4.4
40	UKAM	56.265	162.593	1.5 ± 2.1	−0.3 ± 1.7	2.8 ± 6.7
41	UKR3	44.026	145.865	−2.6 ± 5.1	−2.1 ± 5.0	8.2 ± 21.4
42	VODO	51.809	158.077	1532.5 ± 9.8	−1260.5 ± 8.5	−332.1 ± 6.8
43	VSK1	55.660	160.232	5.7 ± 1.2	−26.2 ± 3.0	1.4 ± 4.4
44	YSK1	47.030	142.717	11.2 ± 2.3	3.3 ± 3.1	−1.9 ± 7.9

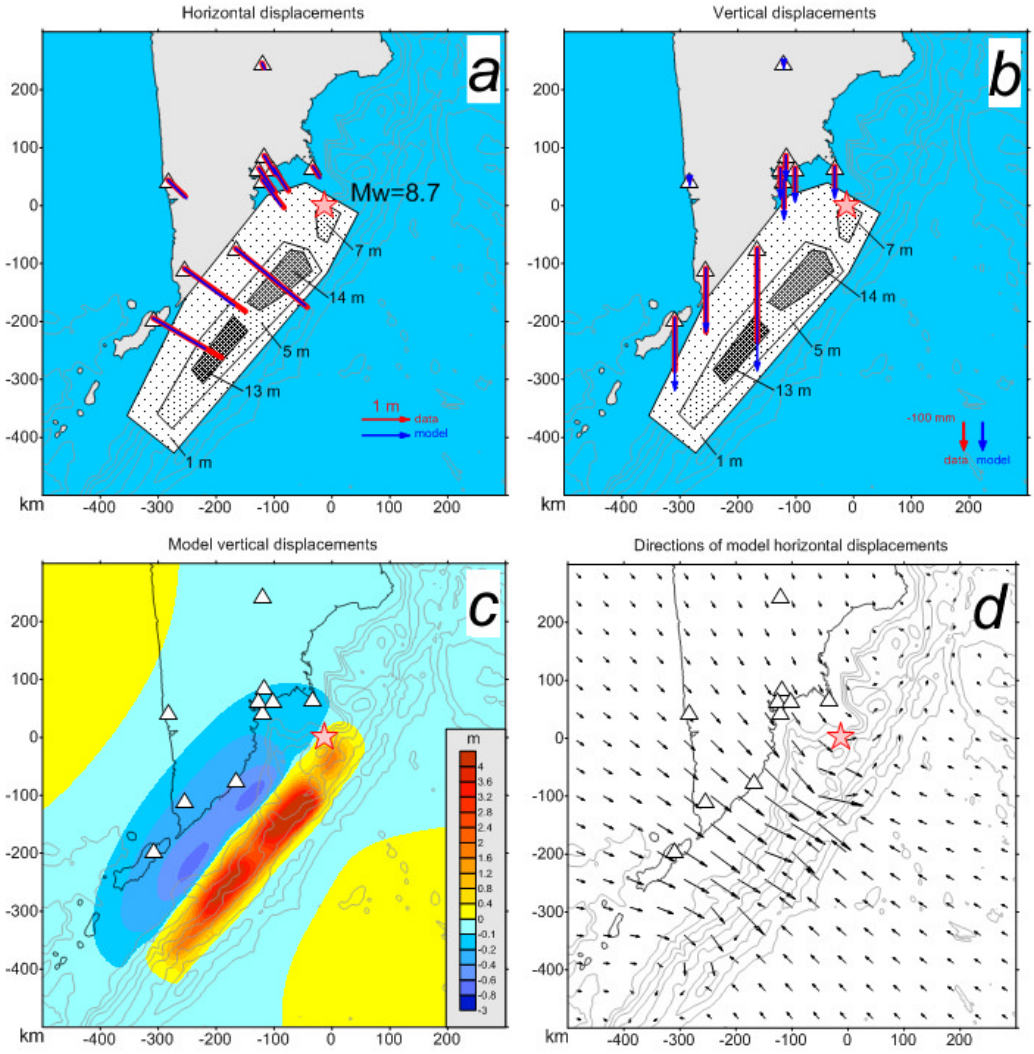

Figure 12. Source model of the Kamchatka earthquake based on coseismic displacement data. Figures *a* and *b* show the projection of the model source point onto the ground surface and a comparison of the measured (red lines or arrows) and modeled (blue) displacements for each of the stations used (shown as triangles). Model source displacement values are shown in black font in *a* and *b*. Figures *c* and *d* show maps of the modeled ground surface displacement for the entire specified area in the vicinity of the source point. The star is the epicenter of the mainshock.

developed by the branch's specialists [*Mityushkina et al.*, 2011]. Information on earthquake shaking perceptions comes both directly from the population and is entered by specialists of the KB GS RAS based on telephone survey results and radiograms. The assessment of macroseismic intensity I is determined expertly using the criteria of the descriptive part of the Seismic Intensity SIS–17.

Based on the macroseismic information processed as of the time of writing, a preliminary assessment of the intensity of the Kamchatka earthquake's manifestations has been obtained for 46 localities in seven municipalities of Kamchatka Krai (Yelizovsky, Ust-Bolsheretsky, Milkovsky, Sobolevsky, Bystrinsky, Ust-Kamchatsky, and Aleutsky) and the North Kuril District of Sakhalin Oblast. The shaking intensity ranged from 2 to at least 7–8 at epicentral distances of Δ = 91–478 km. The city of Severo-Kurilsk (Δ = 358 km) experienced the greatest macroseismic impact – according to preliminary data, tremors with an intensity of at least 7–8 were observed there; in Petropavlovsk-Kamchatsky, the shaking intensity reached at least 6–7.

Employees of the EMERCOM of Russia, together with specialized organizations engaged under contracts with the administrations of populated areas of Kamchatka Krai and the city of Severo-Kurilsk, conducted surveys of buildings and structures, primarily kindergartens, schools, hospitals, energy and transport facilities, as well as residential buildings, based on requests collected from residents via a specially organized hotline. At the time of writing, the analysis of the collected information is ongoing, and upon its completion, a final assessment of the macroseismic intensity of the Kamchatka earthquake in populated areas may be made. It should be noted that there were no human casualties or significant destruction in any of the populated areas – the majority of surveyed buildings sustained damage of levels 1–2 and were deemed serviceable or limitedly serviceable (after major repairs) for continued use. A preliminary assessment of the macroseismic manifestations of the Kamchatka earthquake is presented in Table 5 and Figure 13.

Table 5. Preliminary assessment of the observed intensity of shaking at points caused by the Kamchatka earthquake in the Kamchatka Krai and the North Kuril District of the Sakhalin Oblast

I, value	Point name (epicentral distance, km)
No less 7–8	Severo-Kurilsk (358)
7	Ozerny cordon (258)
No less 6–7	Cape Shipunsky (91), Petropavlovsk-Kamchatsky (146), Vilyuchinsk (157), MGeoES-1 (159), Nikolaevka (166), Paratunka (168), Termalny (168), Sosnovka (170), Karymshina station (170), Yelozovo (171), HMS Vodopadnaya (178), Razdolny (181)
6	Semyachik (198), Malki (232), Valley of Geysers cordon (233), Pauzhetka (273), Zaporozhye (291), Ozernovsky (292), Cape Chibuyiny (347)
5–6	Vulkanny (168), Cape Lopatka (314)
5	Uzon cordon (241), Aerodrom cordon (244)
4	Sharomy (274), Kavalerskoye (274), Milkovo (289), Ust-Bolsheretsk (292), Oktyabrsky (292), Ipuin cordon (309), Kozyrevsk (413), Klyuchi (441), Ust-Kamchatsk (451)
3–4	Dolinovka (322), Krutoberegovo (456), Nikolskoye (478)
2–3	Ustyevoye (370), Sobolevo (373), Krutogorovsky (440), Cape Afrika (463)
2	Esso (414)
Felt	Krugly lighthouse (154), Svetly (155), Koryaki (187), Atlasovo (366)

According to information collected from the occurrence of the main event through December 31, 2025, 523 felt aftershocks with M_L = 3.5–7.2 and shaking intensities from 1 to 6 were recorded in the source zone. The earthquakes were felt in 79 localities of the Kamchatka Krai and the North Kuril District of Sakhalin Oblast; the cities of Petropavlovsk-Kamchatsky and Severo-Kurilsk experienced macroseismic effects at least 317 and 121 times, respectively. Shaking of intensity up to 6 accompanied the two strongest aftershocks of the Kamchatka earthquake. The first – the September 13 event (M_W = 7.4) – produced intensity I = 6 at Cape Shipunsky (Δ = 33 km) and at the Semyachik hydrometeostation (Δ = 121 km); in Petropavlovsk-Kamchatsky (Δ = 122 km), the shaking did not exceed I = 5. The second – the strongest aftershock recorded on September 18 (M_W = 7.8) – caused shaking of I = 6 at Cape Shipunsky (Δ = 122 km), at the Nalychevo cordon (Δ = 96 km), in Petropavlovsk-Kamchatsky (Δ = 143 km), and in the village of Rybachy (Δ = 152 km); in five other localities (Δ = 119–163 km), the shaking intensity reached 5–6.

2.6. Strong Ground Motion Parameters of the Kamchatka Earthquake

Estimates of strong ground motion parameters for the Kamchatka earthquake (Table 6, Figure 14) were obtained from recordings of the strong motion station network (HN channels) of the KB GS RAS [*Chebrov et al.*, 2013]. Prior to analysis, the recordings were filtered in the frequency band of 0.1–35 Hz [*Chubarova et al.*, 2010]. The instrumental

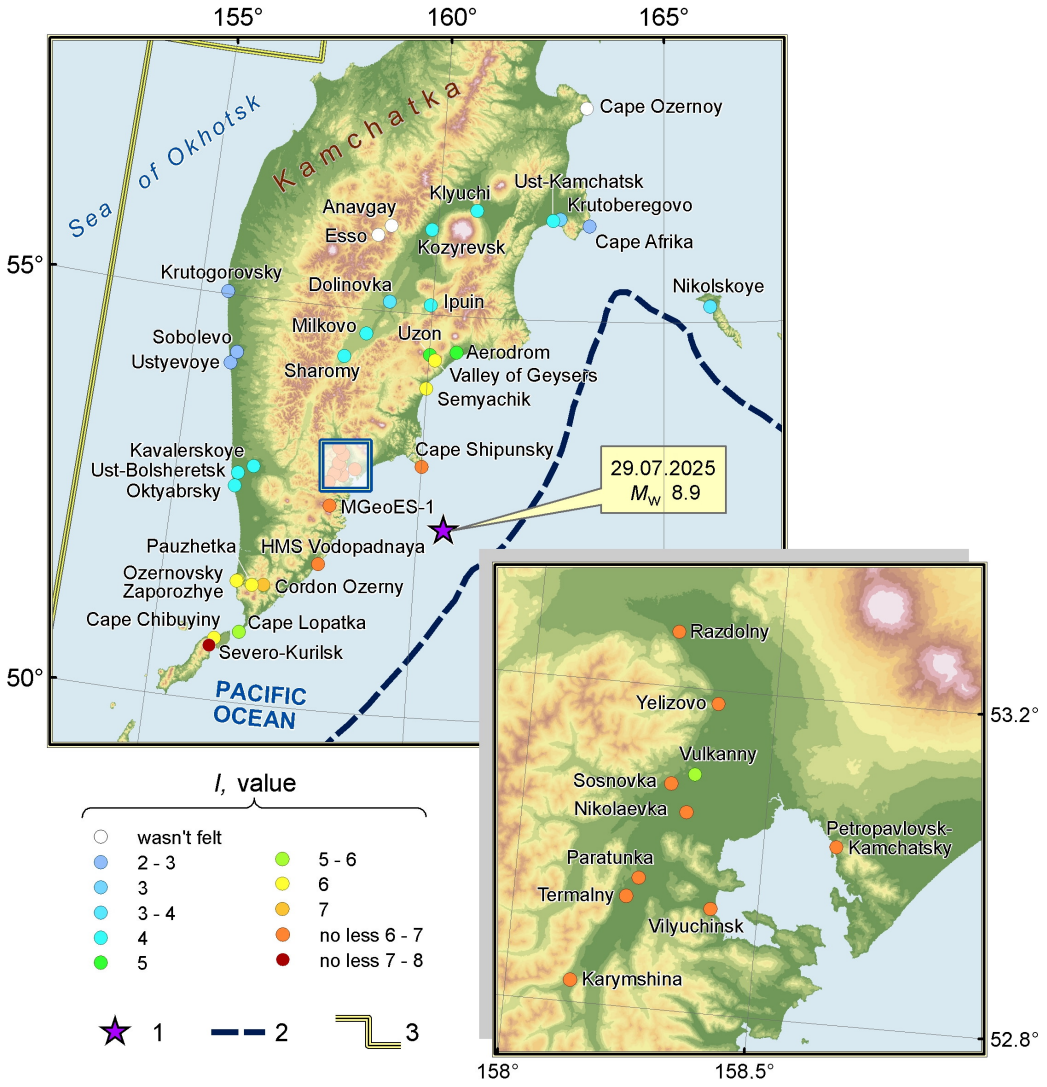

Figure 13. Preliminary assessment of the observed intensity of shaking caused by the Kamchatka earthquake in the Kamchatka Region and the North Kuril District of the Sakhalin Region. 1 – epicenter of the main event; 2 – deep-sea trench; 3 – boundaries of the responsibility area of the KB GS RAS.

intensity I_a was calculated using the formula $I_a = 2.5\lg(a_{peak}) + 1.89$ (SIS–17), where a_{peak} (cm/s^2) is the peak acceleration on the horizontal channels.

At 38 stations, ground accelerations exceeding 1 cm/s^2 were recorded; at 27 stations, they exceeded 40 cm/s^2. It should be noted that acceleration values increased with distance southwest of the epicenter, which may be explained by directivity effects of rupture propagation. At station SPN, the closest to the epicenter (Δ = 91 km), the ground acceleration was only one-fifth of the peak acceleration recorded at station SKR (Δ = 358 km). At a distance of 1,425 km southwest of the epicenter, at the YUK station, the recorded acceleration was more than twice the value recorded at the BKI station, located 478 km to the northeast.

3. Conclusion

The Kamchatka earthquake of July 29, 2025 (M_W = 8.9), one of the strongest seismic events recorded in the world during the instrumental period, occurred in the upper layer ($0 \le h \le 70$ km) of the Kamchatka seismic focal zone, whose extremely high seismicity is associated with the subduction process of the Pacific Plate beneath the Okhotsk Plate. The subduction nature of the earthquake is confirmed by the mechanisms of the main

Table 6. Parameters of strong ground motions during the Kamchatka earthquake

No.	Station	Δ, km	r, km	a_{peak}, cm/s^2			v_{peak}, cm/s			I_a, value
				Component			Component			
				E	N	Z	E	N	Z	
1	SKR	359	362	−774.78	475.13	−240.6	−42.82	26.29	−6.14	9.1
2	KDT	179	184	439.99	308.19	219.26	−20.42	14.29	9.49	8.5
3	RUS	137	144	−221.43	172.92	−138.06	12.53	−10.26	−7.94	7.8
4	MSN	149	155	−232.71	−236.33	152.91	−21.75	−33.86	10.11	7.8
5	KRM	171	176	−229.83	−163.01	90.44	12.50	−9.89	−6.20	7.8
6	GK004	147	154	−159.92	181.89	−154.8	7.18	−9.12	−4.53	7.5
7	RIB	149	155	−137.32	159.83	53.84	−13.61	−12.45	3.93	7.4
8	SPZ	148	154	−149.1	98.6	−52.12	−16.01	9.46	−4.94	7.3
9	NIC	167	172	−145.64	129.08	28.13	−16.90	−12.68	−3.14	7.3
10	SPN	90	100	132.24	136.95	−101.29	−357.31	−252.23	−739.42	7.2
11	NLC	121	128	−93.18	−135.5	41.22	−13.08	15.41	2.90	7.2
12	VIL	157	163	82.48	−121.7	80.58	−8.42	−11.23	4.88	7.1
13	SCH	142	149	84.03	115.07	37.35	−9.60	−8.93	−3.62	7
14	GK001	142	149	−99.68	−63.68	−31.11	−9.35	5.23	2.71	6.9
15	GK003	150	156	102.22	−103.95	40.39	13.99	12.09	4.68	6.9
16	AER	156	162	−97.83	−84.13	38.6	−12.19	11.13	4.98	6.9
17	PAU	274	278	−90.91	98.79	−61.01	5.68	5.97	−3.53	6.9
18	ADM	147	154	−56.27	−92.1	30.3	−5.50	−5.96	2.83	6.8
19	PTG	150	156	−55.02	−90.75	−58.89	−6.83	−8.35	3.63	6.8
20	GK005	141	148	−58.56	84.44	54.64	−1.31	1.85	1.45	6.7
21	IVS	152	158	−71.54	78.55	39.68	−10.42	−8.52	−4.76	6.6
22	DAL	141	148	−69.98	67.48	42.04	4.61	4.62	−1.98	6.5
23	GK002	144	151	57.54	−65.26	44.51	−3.15	2.82	−2.02	6.4
24	DCH	150	156	51.08	60.9	−28.68	−6.70	6.47	2.79	6.4
25	NII	151	157	58.83	60.53	35.33	−8.23	8.60	4.17	6.4
26	PLVN	172	177	−45.75	−60.3	−30.67	−6.05	−4.08	2.72	6.3
27	PET	147	153	−42.9	−44.12	23.6	−5.16	−3.91	2.83	6
28	TUMD	317	320	14.15	9.23	−6.2	1.76	1.46	0.92	4.8
29	UK5	451	453	7.44	9.67	5.28	3.29	3.70	−1.63	4.4
30	UK4	450	453	9.12	−9.58	4.19	−2.86	−3.71	−1.31	4.3
31	UK1	455	457	8.04	−8.93	4.64	2.46	−2.55	−1.27	4.3
32	UK2	453	455	−7.23	8.03	−3.82	2.82	−3.33	−1.11	4.2
33	KOZ	414	416	−5.06	4.05	−2.33	3.26	2.60	−1.41	3.6
34	YUK	1425	1426	4.35	−4.64	−2.72	0.29	0.20	0.17	3.6
35	KLY	441	443	3.47	−2.94	−1.88	1.87	1.27	−0.83	3.2
36	BKI	478	480	1.18	1.72	−0.89	−0.33	−0.21	0.15	2.5
37	KUR	1219	1220	−1.39	1.63	−0.91	0.40	0.46	0.26	2.4
38	ESO	415	418	−1.14	−1.18	−1.05	−0.51	0.61	−0.65	2.1

Note: The results are presented without corrections for soil and geological conditions. Δ – epicentral distance; r – hypocentral distance; a_{peak} – peak ground acceleration; v_{peak} – peak ground velocity (velocity values were obtained by integrating acceleration records); I_a – instrumental intensity; Z, N, E – channel component orientation (vertical, north-south, east-west).

shock and the majority of the aftershocks, the cloud of which extended more than 500 km along the eastern coast of Kamchatka and the Northern Kuril Islands. The earthquake was preceded by a series of strong events in the Avacha Gulf area, which began after a prolonged quiescence: the Vilyuchinsky earthquake of April 3, 2023 (M_W = 6.6), the

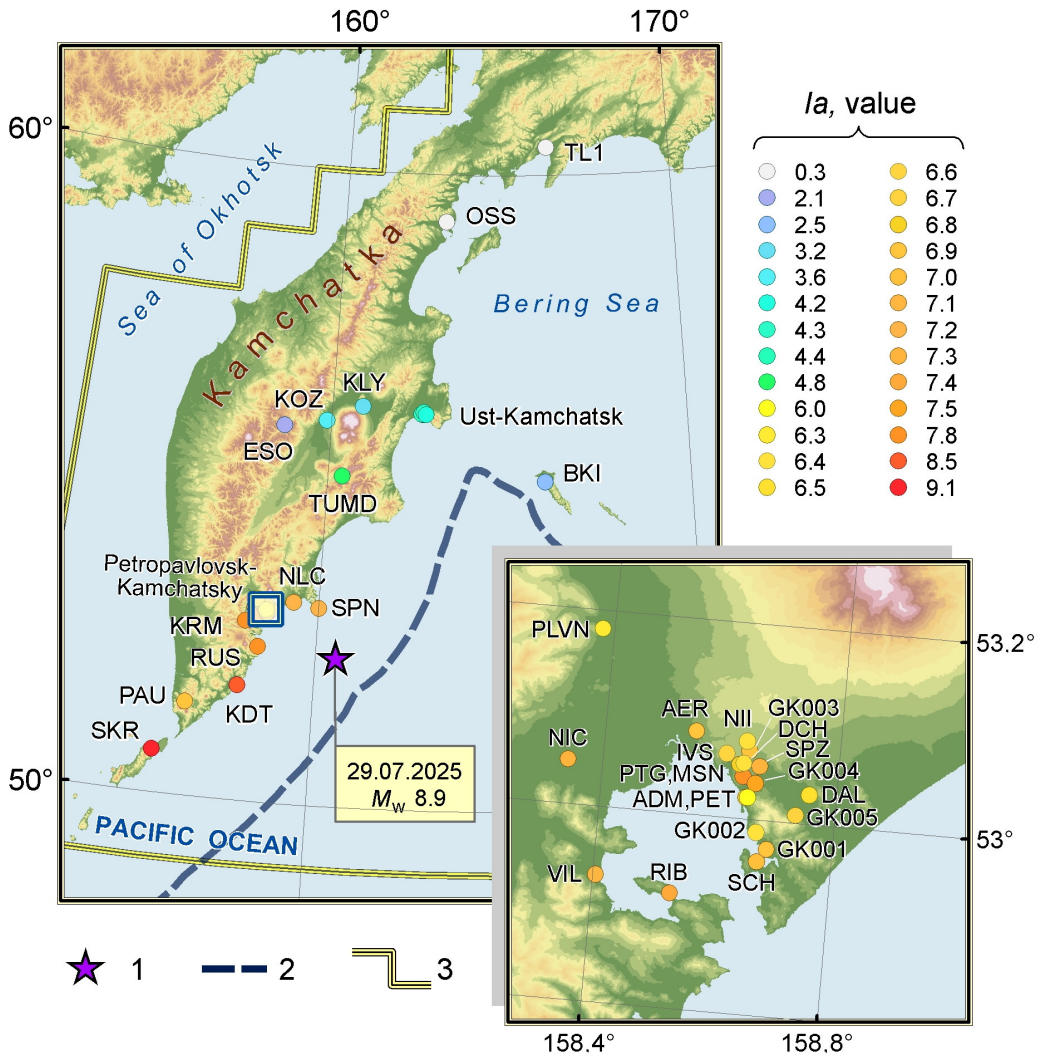

Figure 14. Instrumental shaking intensity calculated based on the parameters of strong ground motions from the Kamchatka earthquake at the stations of the KB GS RAS network and the SKR station of the Sakhalin Branch of GS RAS. 1 – epicenter of the main event; 2 – deep-sea trench; 3 – boundaries of the responsibility area of KB GS RAS.

Shipunsky earthquake of August 17, 2024 (M_W = 7.0), and the Shipunsky-II earthquake of July 20, 2025 (M_W = 7.4).

The Kamchatka earthquake has become the second strongest event of the Kamchatka seismic focal zone in the instrumental period after the Great Kamchatka Earthquake of November 4, 1952 (M_W = 9.0). Striking attention is drawn to the almost complete similarity of the two events in terms of epicenter locations, sizes and configurations of the source areas, and the manifestations of the generated tsunami, which in the case of the Kamchatka earthquake did not lead to catastrophic consequences. Based on the recurrence relationships from [*Gusev and Shumilina*, 2004], the interval between the two events is too short even for the entire Kamchatka seismic focal zone. Furthermore, the 73-year gap between the two strongest earthquakes (M_W = 8.8–9.0) in the same location is significantly shorter than what would be expected from the perspective of seismic cycle theory [*Chebrov*, 2025; *Fedotov*, 1968].

The earthquake was felt over most of the Kamchatka Peninsula, the Commander and Kuril Islands. According to a preliminary assessment of the collected macroseismic information, the shaking intensity ranged from 2 to at least 7–8 at epicentral distances of Δ = 91–478 km. The greatest macroseismic impact was experienced by Severo-

Kurilsk (Δ = 358 km) – shaking with an intensity of at least 7–8 were observed there; in Petropavlovsk-Kamchatsky, the intensity reached at least 6–7. The powerful tsunami generated by the Kamchatka earthquake was most pronounced along the southern part of the eastern coast of Kamchatka and the Northern Kuril Islands, where wave heights exceeded 15 m. In Severo-Kurilsk, the port and the fish processing plant buildings located on the shore were flooded. It should be noted that despite the exceptional strength of the earthquake, the large extent of its source, and its proximity to populated areas, the Kamchatka earthquake and the associated tsunami caused no human casualties or serious destruction. For most buildings surveyed after the earthquake in the populated areas of Kamchatka and the city of Severo-Kurilsk, damage of levels 1–2 was recorded, which allows them to be classified as serviceable or limitedly serviceable (after major repairs) for continued use. In Severo-Kurilsk, which experienced the greatest impact from the tsunami, a timely warning of the tsunami threat was issued, allowing residents to evacuate in advance to the hills surrounding the city.

The Kamchatka earthquake triggered an extremely powerful aftershock process that is still ongoing. By December 31, 2025, the KB GS RAS had produced an aftershock catalog containing the main parameters of 3,801 events in the range M_L = 1.7–7.2, selected from approximately 30,000 earthquakes detected by the automatic single-station detection system. The completeness of the resulting catalog, including the main event, at the time of writing is estimated as M_L^C = 5.6, which is significantly higher than the completeness magnitude of the general Kamchatka earthquake catalog (M_L^C = 3.5), and is still insufficient for a detailed assessment of the aftershock process.

Six events of the aftershock sequence had a magnitude of $M_W \geq 6.1$. The two strongest among them were recorded in the Pacific Ocean near Cape Shipunsky on September 13, 2025 (M_W = 7.4) and September 18, 2025 (M_W = 7.8). The maximum observed shaking intensity of I = 6 for both earthquakes was recorded at Cape Shipunsky, while in Petropavlovsk-Kamchatsky it reached 5 and 5–6, respectively. In the source zone, 523 felt aftershocks with M_L = 3.5–7.2 and shaking intensities from 1 to 6 were recorded across the Kamchatka Krai and the North Kuril District of Sakhalin Oblast. The cities of Petropavlovsk-Kamchatsky and Severo-Kurilsk experienced macroseismic effects at least 317 and 121 times, respectively. The main event exceeded the strongest aftershock by ΔM_W = 1.1, which is consistent with Båth's law. The source size, estimated from the aftershock cloud, is 580 × 180 km.

To identify patterns of the aftershock process under conditions of a scarcity of small earthquakes in the catalog, an analysis of the daily variation of seismic energy released since the occurrence of the main event was applied. Previously, all earthquakes in the aftershock catalog were converted to an equivalent moment magnitude scale. As a result, two phases of the source process development were identified, characterized by significantly different energy release regimes, separated by the strongest aftershocks on September 13 and 18 with M_W = 7.4 and 7.8. A change in the regime after the strongest aftershocks has been repeatedly noted in global practice, including for earthquakes in the Kamchatka region. Also worth mentioning is the swarm activation that occurred in the Pacific Ocean opposite Avacha Gulf on November 3 and 4, 2025. The total energy of this swarm corresponds to a magnitude M_W = 6.4, which allows it to be considered the strongest event during the relaxation in the source – the second phase of the source process development.

As of December 31, 2025, the operative catalog of seismic moment tensors was received in the KB GS RAS for the main event and for 97 earthquakes of the aftershock sequence with M_W = 4.7–7.8, based on recordings from broadband seismic stations in Kamchatka, the Russian Far East, Alaska, and Japan. From the moment tensor parameters, focal mechanisms, scalar seismic moment values, and moment magnitudes M_W were calculated. The obtained results are in good agreement with the determinations from global catalogs (GCMT and NEIC). An analysis of the distribution of source mechanism types for the aftershocks showed that the majority (74%) are reverse faults, like the main event, and are close to its mechanism in terms of the orientation of the principal axes.

According to data from the Global Navigation Satellite System, the Kamchatka earthquake caused significant coseismic displacements of the Earth's surface on the Kamchatka Peninsula, the western coast of the Sea of Okhotsk, the Kuril Islands, and Sakhalin Island. The largest horizontal displacements, reaching up to 2 m, were recorded in the south of the Kamchatka Peninsula and on Paramushir Island, in the area of maximum slip along the fault surface. Based on the horizontal and vertical displacement components at ten GNSS stations closest to the source and having the smallest relative errors, A. V. Lander constructed a source model of the Kamchatka earthquake. According to the model, the source dimensions reached approximately 520 × 160 km, and the maximum source slip reached 14 m.

The Kamchatka earthquake is the strongest event recorded by the regional network of seismic stations since its inception in 1961, and it can rightfully be called a stress test that was successfully passed both by the observation system of the KB GS RAS and by its staff. Kamchatka seismologists demonstrated the highest level of professionalism, composure, and courage – the rapid processing of the main event and the issuance of the tsunami warning by the staff of the Petropavlovsk Regional Data Processing Center was completed within the regulation-mandated seven minutes, under conditions of shaking of intensity up to 6–7 that lasted for the first four minutes. In the following months, amid a developing aftershock sequence with numerous felt earthquakes that caused shaking of up to 6 in Petropavlovsk-Kamchatsky, the branch's specialists continued to perform their official duties, remaining at their workplaces even during strong tremors. The staff of the KB GS RAS, who participated in the rapid and final processing of earthquakes and the determination of their additional parameters, were awarded medals from the EMERCOM of Russia "For Partnership in the Name of Salvation" and Certificates of Honor from EMERCOM and the Government of Kamchatka Krai.

The primary task of the KB GS RAS remains the compilation of final catalogs of earthquakes of the aftershock sequence, focal mechanisms and source parameters, as well as the macroseismic catalog, as necessary source material for a detailed analysis of the source process and expanding understanding of the seismicity, geodynamics, and tectonics of the Kamchatka seismic focal zone. The results obtained will be of great importance for refining the assessment of seismic and tsunami hazards in the northwestern Pacific region and for identifying patterns of source processes of the largest earthquakes in general.

Acknowledgments. This work was supported by the Ministry of Science and Higher Education of the Russian Federation through state assignments Nos. 124020900029-7 and 075-00609-26. The data used in the work were obtained with large-scale research facilities "Seismic Infrasound Array for Monitoring of the Russian Federation, Neighbouring Territories and the World". The study employed waveform data from the F-net network, operated by NIED (National Research Institute for Earth Science and Disaster Prevention, Japan), and the global network of seismic stations downloaded via the Wilber 3 system (https://ds.iris.edu/wilber3) of the IRIS consortium (Incorporated Research Institutions for Seismology).

Appendix A

Table A1. Operative catalog of mechanisms and parameters of the sources of the Kamchatka earthquake and its aftershocks, obtained at the KB GS RAS using the RSMT method as of December 31, 2025

No.	Date, time	$\varphi°$, N	$\lambda°$, E	h, km	M_L	T		N		P		NP1			NP2			h_e, km	τ, s	p	M_0, 10^pN·m	M_W	n	ε, %
						pl°	az°	pl°	az°	pl°	az°	strk°	dip°	slp°	strk°	dip°	slp°							
1	2	3	4	5	6	7	8	9	10	11	12	13	14	15	16	17	18	19	20	21	22	23	24	25
1	29.07.2025 23:24	52.36	160.53	25	7.5	61	309	3	213	29	122	203	16	79	34	74	93	25	224	22	2.91	8.9	12	21
2	30.07.2025 0:16	52.15	159.58	20	6.7	69	345	12	220	16	126	198	31	65	46	62	104	20	12	19	2.22	6.8	8	17
3	30.07.2025 5:05	50.68	157.87	20	5.9	10	145	6	54	79	295	242	36	−80	50	55	−97	20	0	16	8.7	5.2	8	21
4	30.07.2025 5:19	51.34	158.88	30	6.1	19	316	12	222	67	102	217	66	−103	66	28	−63	30	0	17	2.09	5.5	10	21
5	30.07.2025 9:56	51.54	159.82	15	5.9	75	234	15	35	5	126	232	42	112	23	52	71	15	6	18	1.03	5.9	11	18
6	30.07.2025 11:38	50.98	158.33	15	5.9	6	300	33	34	57	201	359	48	−136	236	59	−51	15	0	16	3.67	5	9	21
7	30.07.2025 12:01	51.00	158.97	5	5.9	42	312	2	44	48	136	224	87	−88	9	4	−125	5	0	16	7.83	5.2	8	13
8	30.07.2025 12:44	49.42	158.07	15	6	75	270	11	42	11	134	238	35	108	35	57	77	15	0	17	1.97	5.5	12	24
9	30.07.2025 14:47	50.05	157.82	15	6.4	10	150	14	242	73	27	223	38	−114	72	56	−73	15	0	17	8.02	5.9	12	12
10	30.07.2025 16:57	49.95	157.74	20	6.1	27	74	46	314	32	183	310	86	−136	216	46	−5	20	2	17	2.12	5.5	14	23
11	30.07.2025 17:20	51.32	159.67	15	6.1	81	303	1	40	9	130	221	36	92	39	54	89	15	2	16	7.01	5.2	9	17
12	30.07.2025 23:15	52.37	160.94	5	6.1	40	276	6	12	49	109	317	8	−145	192	86	−84	5	0	17	4.73	5.7	8	26
13	31.07.2025 2:38	51.58	160.29	15	5.8	81	353	7	215	6	124	206	39	79	41	52	99	15	8	17	1.31	5.3	6	18

Continued on next page

Table A1. Operative catalog of mechanisms and parameters of the sources of the Kamchatka earthquake and its aftershocks, obtained at the KB GS RAS using the RSMT method as of December 31, 2025(Continued)

No.	Date, time	$\varphi°$, N	$\lambda°$, E	h, km	M_L	T		N		P		NP1			NP2			h_e, km	τ, s	p	M_0, 10^pN·m	M_W	n	ε, %
						pl°	az°	pl°	az°	pl°	az°	strk°	dip°	slp°	strk°	dip°	slp°							
1	2	3	4	5	6	7	8	9	10	11	12	13	14	15	16	17	18	19	20	21	22	23	24	25
14	31.07.2025 5:27	49.60	158.82	5	6.7	8	128	25	222	64	21	192	42	−128	59	58	−61	5	8	18	2.45	6.2	13	12
15	31.07.2025 7:42	49.85	157.73	10	5.9	40	20	19	273	43	163	272	88	−109	178	19	−5	10	2	16	7.22	5.2	12	20
16	31.07.2025 14:29	51.53	159.81	15	5.8	77	302	2	39	13	129	221	32	93	38	58	88	15	6	16	5.95	5.1	6	17
17	31.07.2025 14:35	50.84	158.83	5	6.2	48	297	4	203	42	109	151	5	38	23	87	94	5	4	17	2.42	5.5	7	47
18	31.07.2025 18:40	51.48	159.75	15	5.9	70	297	3	35	20	126	221	25	97	33	65	87	15	8	16	3.37	5	10	22
19	31.07.2025 20:36	52.50	161.14	10	5.9	67	303	2	38	23	129	223	22	95	37	68	88	10	0	17	3.38	5.6	12	16
20	01.08.2025 8:34	52.64	160.14	40	5.8	69	287	8	38	19	130	234	26	108	34	65	81	40	0	17	4.6	5.7	10	11
21	01.08.2025 10:54	50.65	157.80	15	5.8	15	132	6	40	73	288	231	30	−77	37	61	−97	15	10	17	4.24	5.7	11	16
22	01.08.2025 11:57	51.75	160.11	10	6.2	86	2	3	215	2	125	211	43	85	38	47	95	10	4	17	5.81	5.8	10	24
23	01.08.2025 12:39	51.29	161.19	15	6.1	74	327	4	223	16	132	216	30	82	45	61	94	15	0	17	1.2	5.3	7	37
24	01.08.2025 13:44	51.83	158.70	60	6.1	74	282	6	34	15	126	225	30	103	30	60	83	60	0	17	2.98	5.6	12	14
25	01.08.2025 16:36	50.92	158.24	25	5.8	9	114	15	22	73	235	221	38	−66	11	56	−108	25	0	16	6.53	5.1	8	7
26	01.08.2025 18:20	50.25	159.08	5	6.2	10	311	25	46	63	200	241	60	−61	14	41	−130	5	10	18	1.52	6.1	12	13
27	01.08.2025 20:07	50.30	156.58	60	6.3	71	296	4	38	18	130	226	27	99	36	64	85	60	0	17	1.09	5.3	11	19
28	02.08.2025 11:05	51.38	159.88	15	6.2	78	300	2	37	12	127	219	33	93	36	57	88	15	0	17	1.27	5.3	12	20

Continued on next page

Table A1. Operative catalog of mechanisms and parameters of the sources of the Kamchatka earthquake and its aftershocks, obtained at the KB GS RAS using the RSMT method as of December 31, 2025(Continued)

No.	Date, time	$\varphi°$, N	$\lambda°$, E	h, km	M_L	T		N		P		NP1			NP2			h_e, km	τ, s	p	M_0, 10^pN·m	M_W	n	ε, %
						pl°	az°	pl°	az°	pl°	az°	strk°	dip°	slp°	strk°	dip°	slp°							
1	2	3	4	5	6	7	8	9	10	11	12	13	14	15	16	17	18	19	20	21	22	23	24	25
29	02.08.2025 14:14	51.49	159.82	15	6.3	79	314	2	216	11	126	214	34	87	37	56	92	15	0	17	9.13	5.9	11	16
30	03.08.2025 5:37	50.48	157.97	25	6.9	5	137	10	228	79	20	216	41	−106	56	51	−77	25	4	19	1.31	6.7	11	14
31	03.08.2025 14:26	52.26	160.99	5	6.2	8	143	4	52	81	296	237	37	−84	49	53	−95	5	8	17	2.73	5.6	12	20
32	03.08.2025 18:07	52.31	161.14	10	6	64	244	24	36	11	131	247	40	129	21	60	62	10	0	17	2.52	5.5	8	12
33	04.08.2025 6:48	49.54	157.15	15	5.8	53	332	1	240	37	149	230	8	80	60	82	91	15	6	16	1.59	4.7	8	16
34	06.08.2025 5:01	50.02	158.78	5	5.8	9	307	22	40	66	195	235	58	−64	13	41	−125	5	6	16	5.3	5.1	12	23
35	06.08.2025 10:35	51.43	159.71	15	6.3	77	276	7	36	11	128	226	34	102	32	57	82	15	0	17	4.18	5.7	12	21
36	09.08.2025 14:04	50.08	159.85	10	6.3	10	308	0	38	80	130	218	55	−90	37	35	−91	10	0	18	1.18	6	13	15
37	10.08.2025 6:59	51.34	159.81	10	5.9	70	320	4	218	19	126	209	26	80	40	65	95	10	2	16	6.31	5.1	8	19
38	11.08.2025 17:25	50.20	157.21	30	5.9	26	318	3	49	64	146	230	71	−87	41	20	−99	30	0	16	4.12	5	12	17
39	15.08.2025 10:11	52.80	159.97	50	6.2	72	288	6	35	18	127	225	28	102	32	63	84	50	0	17	4.62	5.7	11	13
40	19.08.2025 14:41	49.36	155.76	50	5.9	9	172	27	266	62	65	233	43	−131	104	59	−58	50	0	16	2.79	4.9	11	15
41	21.08.2025 11:21	51.68	160.39	15	6	66	242	20	27	12	122	236	37	125	15	60	67	15	4	17	4.9	5.7	10	21
42	23.08.2025 3:44	50.77	157.40	50	5.9	70	281	9	38	17	131	235	29	109	33	63	80	50	0	17	2.19	5.5	12	14
43	23.08.2025 21:29	51.98	160.81	15	5.8	78	237	11	34	5	124	227	41	107	24	51	75	15	0	17	1.41	5.4	9	16

Continued on next page

Table A1. Operative catalog of mechanisms and parameters of the sources of the Kamchatka earthquake and its aftershocks, obtained at the KB GS RAS using the RSMT method as of December 31, 2025(Continued)

No.	Date, time	$\varphi°$, N	$\lambda°$, E	h, km	M_L	T		N		P		NP1			NP2			h_e, km	τ, s	p	M_0, 10^pN·m	M_W	n	ε, %
						pl°	az°	pl°	az°	pl°	az°	strk°	dip°	slp°	strk°	dip°	slp°							
1	2	3	4	5	6	7	8	9	10	11	12	13	14	15	16	17	18	19	20	21	22	23	24	25
44	25.08.2025 6:48	49.53	160.29	10	6.5	16	316	2	226	74	130	225	61	−92	49	29	−87	10	4	18	1.92	6.1	11	23
45	25.08.2025 22:13	49.01	157.03	10	6.1	65	298	4	35	24	127	225	21	100	34	70	86	10	2	17	2.95	5.6	9	25
46	27.08.2025 3:49	50.62	157.68	45	6.2	71	338	5	232	18	141	222	27	78	55	64	96	45	0	18	1.07	6	11	9
47	02.09.2025 11:25	52.59	160.61	15	5.8	70	304	4	45	20	137	234	26	100	44	65	85	15	4	16	6.69	5.2	9	11
48	03.09.2025 3:38	51.25	160.00	10	5.8	72	325	6	217	17	126	207	28	78	40	62	96	10	4	17	1.06	5.3	8	24
49	04.09.2025 22:38	52.26	160.94	15	5.9	81	277	4	35	8	126	221	37	97	32	53	85	15	4	17	1.04	5.3	10	16
50	08.09.2025 8:26	52.29	161.01	15	5.8	79	314	2	216	11	126	214	34	87	37	56	92	15	2	16	7.72	5.2	10	17
51	10.09.2025 18:03	51.43	159.79	15	5.8	63	247	21	28	15	124	241	35	129	17	63	66	15	2	16	3.75	5	6	11
52	13.09.2025 2:37	53.03	160.48	50	6.9	74	319	4	215	15	124	209	30	82	38	60	94	50	22	20	1.33	7.4	17	16
53	13.09.2025 6:22	52.99	160.89	40	5.8	77	289	4	35	12	126	221	33	97	33	57	86	40	0	17	1.67	5.4	9	9
54	15.09.2025 0:06	53.08	160.18	45	5.8	71	303	3	42	19	134	229	27	98	41	64	86	45	0	16	8.55	5.2	10	11
55	15.09.2025 16:34	52.63	160.96	15	5.9	77	295	3	38	13	129	223	32	96	36	58	86	15	0	17	7.73	5.9	10	13
56	17.09.2025 20:57	52.45	159.48	45	5.9	63	121	9	12	25	277	347	22	64	195	70	100	45	0	17	1.82	5.4	12	21
57	18.09.2025 18:58	53.12	160.78	35	7.2	74	279	5	28	15	119	217	31	100	25	60	84	35	40	20	5.7	7.8	18	21
58	18.09.2025 21:37	52.69	161.36	15	6.1	84	303	0	36	6	126	217	39	91	36	51	90	15	0	17	2.6	5.5	5	26

Continued on next page

Table A1. Operative catalog of mechanisms and parameters of the sources of the Kamchatka earthquake and its aftershocks, obtained at the KB GS RAS using the RSMT method as of December 31, 2025(Continued)

No.	Date, time	$\varphi°$, N	$\lambda°$, E	h, km	M_L	T		N		P		NP1			NP2			h_e, km	τ, s	p	M_0, 10^pN·m	M_W	n	ε, %
						pl°	az°	pl°	az°	pl°	az°	strk°	dip°	slp°	strk°	dip°	slp°							
1	2	3	4	5	6	7	8	9	10	11	12	13	14	15	16	17	18	19	20	21	22	23	24	25
59	19.09.2025 13:27	52.15	160.60	15	5.9	87	319	0	223	3	133	223	42	90	44	48	90	15	4	17	1.74	5.4	11	24
60	19.09.2025 14:55	51.10	158.15	50	6.1	70	275	9	30	17	123	226	29	108	26	63	80	50	0	17	9.12	5.9	12	12
61	19.09.2025 15:45	52.78	161.43	15	6	77	245	11	28	8	120	222	38	107	20	54	77	15	0	17	7.99	5.9	11	15
62	19.09.2025 17:06	52.78	161.43	15	5.9	73	324	1	230	17	140	228	28	87	51	62	91	15	2	16	9.39	5.2	10	23
63	20.09.2025 2:47	52.92	160.18	50	5.9	71	291	1	25	19	115	208	26	93	24	64	88	50	0	16	7.45	5.2	10	26
64	21.09.2025 1:13	52.74	161.29	15	6.1	69	309	1	42	21	132	225	24	93	42	66	89	15	0	17	2.5	5.5	11	27
65	22.09.2025 16:28	51.47	159.66	10	6.2	66	314	2	218	24	127	212	21	83	39	69	93	10	4	17	1.61	5.4	11	27
66	22.09.2025 17:13	51.44	159.70	15	5.8	77	345	7	221	11	130	211	35	77	46	56	99	15	6	16	8.41	5.2	10	18
67	22.09.2025 18:18	51.41	159.75	15	6	77	299	1	36	13	126	218	32	93	35	58	88	15	2	17	2.78	5.6	11	18
68	22.09.2025 18:46	51.43	159.83	15	5.8	80	338	5	220	9	129	213	36	81	43	54	96	15	4	17	1.07	5.3	8	11
69	25.09.2025 9:59	52.04	160.49	20	5.8	78	287	7	52	10	143	241	36	102	47	55	82	20	0	16	7.63	5.2	10	15
70	29.09.2025 22:07	52.86	160.02	45	6.1	68	286	9	37	20	131	236	26	110	34	66	81	45	0	17	2.12	5.5	8	14
71	03.10.2025 16:07	51.46	160.23	15	6.2	81	264	6	34	7	125	222	39	99	30	52	83	15	4	18	1.03	5.9	12	23
72	09.10.2025 13:28	51.53	158.48	50	6.1	71	332	6	226	19	134	215	27	78	49	64	96	50	0	18	1.55	6.1	12	11
73	10.10.2025 11:15	50.23	156.54	60	5.8	73	288	5	33	17	125	222	29	100	31	62	84	60	0	16	9.29	5.2	6	9

Continued on next page

Table A1. Operative catalog of mechanisms and parameters of the sources of the Kamchatka earthquake and its aftershocks, obtained at the KB GS RAS using the RSMT method as of December 31, 2025(Continued)

No.	Date, time	$\varphi°$, N	$\lambda°$, E	h, km	M_L	T		N		P		NP1			NP2			h_e, km	τ, s	p	M_0, 10^pN·m	M_W	n	ε, %
						pl°	az°	pl°	az°	pl°	az°	strk°	dip°	slp°	strk°	dip°	slp°							
1	2	3	4	5	6	7	8	9	10	11	12	13	14	15	16	17	18	19	20	21	22	23	24	25
74	11.10.2025 3:08	53.11	160.13	55	6.1	77	316	2	215	13	125	212	33	86	37	58	93	55	0	17	1.31	5.3	8	14
75	11.10.2025 12:25	50.25	156.65	55	6.3	72	275	10	37	15	130	235	31	110	32	61	78	55	0	17	5.2	5.7	10	21
76	17.10.2025 1:25	53.07	160.19	50	5.9	72	309	1	214	18	124	211	27	87	35	63	92	50	0	16	6.17	5.1	9	10
77	21.10.2025 23:37	52.50	159.14	60	5.6	78	295	2	36	12	126	219	33	94	34	57	87	60	0	16	5.9	5.1	7	15
78	23.10.2025 2:31	51.30	160.00	15	5.9	68	248	18	30	13	125	237	36	122	20	60	69	15	2	17	2.99	5.6	9	17
79	25.10.2025 11:13	49.85	156.33	55	6.2	75	297	2	33	15	124	216	30	93	32	60	88	55	0	17	1.49	5.4	15	15
80	28.10.2025 7:06	50.27	157.84	40	6.1	13	151	19	245	67	28	217	36	−123	76	61	−68	40	0	17	3.03	5.6	11	18
81	03.11.2025 3:55	49.63	156.32	50	5.8	76	296	2	32	14	123	215	31	93	31	59	88	50	0	16	5.42	5.1	7	9
82	03.11.2025 7:10	52.12	160.41	25	6.4	81	289	2	32	9	122	215	36	93	30	54	87	25	10	18	1.07	6	7	37
83	03.11.2025 8:44	52.05	160.62	20	6.4	75	283	6	38	13	130	229	32	102	34	59	82	20	0	18	1.13	6	8	24
84	03.11.2025 19:38	51.65	158.38	50	6.3	67	312	3	48	23	139	235	22	97	47	68	87	50	0	17	1.26	5.3	9	8
85	04.11.2025 3:45	52.10	160.66	25	6.3	79	286	4	39	10	130	226	35	98	36	55	85	25	0	18	1.07	6	9	15
86	04.11.2025 3:58	52.12	160.54	25	5.8	84	291	1	31	6	121	213	39	92	30	51	89	25	2	17	1.15	5.3	6	12
87	04.11.2025 4:45	52.17	160.70	25	6.4	77	287	5	41	12	132	229	33	100	37	57	84	25	0	17	2.35	5.5	9	27
88	04.11.2025 6:28	52.25	160.60	15	6.1	66	302	3	39	24	131	227	21	98	38	69	87	15	0	17	1.63	5.4	10	26

Continued on next page

Table A1. Operative catalog of mechanisms and parameters of the sources of the Kamchatka earthquake and its aftershocks, obtained at the KB GS RAS using the RSMT method as of December 31, 2025(Continued)

No.	Date, time	$\varphi°$, N	$\lambda°$, E	h, km	M_L	T		N		P		NP1			NP2			h_e, km	τ, s	p	M_0, 10^pN·m	M_W	n	ε, %
						pl°	az°	pl°	az°	pl°	az°	strk°	dip°	slp°	strk°	dip°	slp°							
1	2	3	4	5	6	7	8	9	10	11	12	13	14	15	16	17	18	19	20	21	22	23	24	25
89	04.11.2025 23:28	52.06	160.47	20	6.4	78	284	3	32	11	122	217	34	96	29	56	86	20	0	18	1.23	6	10	20
90	04.11.2025 23:49	49.63	156.89	45	6	70	306	1	214	20	123	212	25	88	34	65	91	45	0	17	3.65	5.6	9	11
91	09.11.2025 11:13	51.51	159.79	15	5.8	79	328	4	216	10	126	210	35	82	39	56	95	15	0	16	6.9	5.2	6	9
92	14.11.2025 11:33	50.41	158.41	15	6.1	11	104	43	205	45	3	155	50	−152	46	69	−43	15	0	16	8.69	5.2	9	13
93	21.11.2025 22:38	49.84	158.85	5	6	18	317	15	52	66	179	239	65	−73	23	30	−122	5	2	17	3.13	5.6	6	7
94	07.12.2025 16:34	50.12	156.93	35	6.4	26	319	2	50	64	145	231	71	−87	43	19	−97	35	0	17	3.3	5.6	9	11
95	08.12.2025 1:32	51.27	159.75	15	5.8	79	290	4	42	10	132	227	35	97	39	55	85	15	0	16	4.5	5	7	11
96	12.12.2025 17:43	50.72	157.26	60	6	70	291	5	34	19	126	223	26	101	32	64	85	60	0	16	8.25	5.2	9	12
97	15.12.2025 19:33	51.71	161.19	50	6.3	66	89	12	209	20	304	203	66	76	54	28	118	50	0	17	3.55	5.6	8	11
98	18.12.2025 12:37	52.75	160.08	45	6.4	71	291	5	36	19	127	226	27	102	33	64	84	45	0	17	7.6	5.9	10	10

Note:
1 – earthquake number;
2–6 – data from the earthquake catalog of the KB GS RAS (date and time; latitude φ, longitude λ and depth h of the hypocenter; local magnitude M_L);
7–12 – angles *pl (plunge)*, *az (azimuth)*, defining the orientation of the main axes T, N, P;
13–18 – angles strk, dip, slp, defining the orientation of the mechanism;
19 – h_e – estimate of the depth of the equivalent point source, obtained by calculating the seismic moment tensor;
20– τ – estimate of the duration of the source time function;
21 – p – decimal logarithm of the scaling factor for scalar seismic moment;
22 – scalar seismic moment M_0;
23 – moment magnitude, obtained by recalculation from M_0 using the formula: $M_W = 2/3(\lg(M_0[N \cdot m]) - -9.1)$;
24 – n – number of stations whose records were used in calculations;
25 – ε – residual misfit.

References

Abubakirov I. R., Gusev A. A., Guseva E. M., et al. Mass determination of moment magnitudes MW and establishing the relationship between MW and ML for moderate and small Kamchatka earthquakes // Izvestiya, Physics of the Solid Earth. — 2018. — Vol. 54, no. 1. — P. 33–47. — https://doi.org/10.1134/S1069351318010019

Abubakirov I. R. and Pavlov V. M. Determining the double couple moment tensor for Kamchatka earthquakes from regional seismic waveforms // Izvestiya, Physics of the Solid Earth. — 2021. — Vol. 57, no. 3. — P. 332–347. — https://doi.org/10.1134/S1069351321030010

Båth M. Lateral inhomogeneities of the upper mantle // Tectonophysics. — 1965. — Vol. 2, no. 6. — P. 483–514. — https://doi.org/10.1016/0040-1951(65)90003-X

Chebrov D. V. The Mw = 8.8 Kamchatka megathrust earthquake of july 29, 2025 // Bulletin of Kamchatka Regional Association «Educational-Scientific Center». Earth Sciences. — 2025. — 3(67). — P. 113–117. — https://doi.org/10.31431/1816-5524-2025-3-67-113-117 — (In Russian).

Chebrov D. V., Matveenko E. A., Abubakirov I. R., et al. The MW 7.0 Shipunsky Earthquake of August 17, 2024 off the East Coast of Kamchatka // Journal of Volcanology and Seismology. — 2025a. — Vol. 19, no. 3. — P. 271–280. — https://doi.org/10.1134/S0742046325700101

Chebrov D. V., Matveenko E. A., Abubakirov I. R., et al. Vilyuchinskoye earthquake April 3, 2023 MW 6.6 in Avacha Gulf (Kamchatka) // Vulkanologiya i Sejsmologiya. — 2025b. — No. 6. — P. 31–49. — https://doi.org/10.7868/S3034513825060031 — (In Russian).

Chebrov D. V., Tikhonov S. A., Droznin D. V., et al. Kamchatka seismic monitoring and Earthquake prediction system and its evolution. Main results of observations in 2016-2020 // Russian Journal of Seismology. — 2021. — Vol. 3, no. 3. — P. 28–49. — https://doi.org/10.35540/2686-7907.2021.3.02 — (In Russian).

Chebrov V. N. Expansion of the system of the seismological observations for tsunami warning in Far East of Russia // Bulletin of Kamchatka Regional Association «Educational-Scientific Center». Earth Sciences. — 2007. — 1(9). — P. 27–36. — (In Russian).

Chebrov V. N., Drozhin D. V., Kugaenko Yu. A., et al. The system of detailed seismological observations in Kamchatka in 2011 // Journal of Volcanology and Seismology. — 2013. — Vol. 7, no. 1. — P. 16–36. — https://doi.org/10.1134/S0742046313010028

Chebrov V. N., Drozhina S. Ya., Senyukov S. L., et al. Kamchatka and Komandor Islands // The earthquakes of Russia in 2013. — Obninsk : GS RAS, 2015. — P. 58–65. — (In Russian).

Chubarova O. S., Gusev A. A. and Chebrov V. N. The ground motion excited by the Olyutorskii earthquake of April 20, 2006 and by its aftershocks based on digital recordings // Journal of Volcanology and Seismology. — 2010. — Vol. 4, no. 2. — P. 126–138. — https://doi.org/10.1134/s0742046310020065

Droznin D. V., Chebrov D. V., Droznina S. Ya., et al. Automated estimation of seismic shaking intensity from instrumental data in quasi-real-time mode and its use in the operation of the Seismic Early Warning Service in the Kamchatka Region // Seismic Instruments. — 2018. — Vol. 54, no. 3. — P. 239–246. — https://doi.org/10.3103/S0747923918030088

Droznin D. V. and Droznina S. Y. Interactive DIMAS program for processing seismic signals // Seismic Instruments. — 2011. — Vol. 47, no. 3. — P. 215–224. — https://doi.org/10.3103/s0747923911030054

Dziewonski A. M., Chou T.-A. and Woodhouse J. H. Determination of earthquake source parameters from waveform data for studies of global and regional seismicity // Journal of Geophysical Research: Solid Earth. — 1981. — Vol. 86, B4. — P. 2825–2852. — https://doi.org/10.1029/JB086iB04p02825

Ekström G., Nettles M. and Dziewoński A. M. The global CMT project 2004-2010: Centroid-moment tensors for 13,017 earthquakes // Physics of the Earth and Planetary Interiors. — 2012. — Vol. 200/201. — P. 1–9. — https://doi.org/10.1016/j.pepi.2012.04.002

Fedotov S. A. On the seismic cycle, possibilities of quantitative seismic zonation, and long-term earthquake prediction // Seismic Zoning of the USSR. — Moscow : Nauka, 1968. — P. 121–150. — (In Russian).

Fedotov S. A. Energy classification of Kuril-Kamchatka earthquakes and the problem of magnitudes. — Moscow : Nauka, 1972. — 116 p. — (In Russian).

Gordeev E. I., Fedotov S. A. and Chebrov V. N. Main results of seismological studies in Kamchatka based on detailed observations in 1961-2011 // Seismological and geophysical studies in Kamchatka. Dedicated to 50th anniversary of regional seismological research. — Petropavlovsk-Kamchatsky : Novaya Kniga, 2012. — P. 9–35. — (In Russian).

Gordeev E. I., Levina V. I., Chebrov V. N., et al. Earthquakes of Kamchatka and the Commander Islands // Earthquakes of Northern Eurasia in 1993. — Moscow : GS RAN, 1999. — P. 102–114. — (In Russian).

Gospodinov D. and Rotondi R. Statistical Analysis of Triggered Seismicity in the Kresna Region of SW Bulgaria (1904) and the Umbria-Marche Region of Central Italy (1997) // Pure and Applied Geophysics. — 2006. — Vol. 163, no. 8. — P. 1597–1615. — https://doi.org/10.1007/s00024-006-0084-4

Gusev A. A. The schematic map of the source zones of large Kamchatka earthquakes of the instrumental epoch // Complex seismological and geophysical researches of Kamchatka. To 25th Anniversary of Kamchatkan Experimental & Methodical Seismological Department. — Petropavlovsk-Kamchatsky : GS RAS, 2004. — P. 75–80. — (In Russian).

Gusev A. A. and Shumilina L. S. Recurrence of Kamchatka strong earthquakes on a scale of moment magnitudes // Izvestiya, Physics of the Solid Earth. — 2004. — Vol. 40, no. 3. — P. 206–215.

Gutenberg B. The energy of earthquakes // Quarterly Journal of the Geological Society of London. — 1956. — Vol. 112, no. 1–4. — P. 1–14. — https://doi.org/10.1144/gsl.jgs.1956.112.01-04.02

Kagan Y. Simplified algorithms for calculating double-couple rotation // Geophysical Journal International. — 2007. — Vol. 171, no. 1. — P. 411–418. — https://doi.org/10.1111/j.1365-246X.2007.03538.x

Kanamori H. The energy release in great earthquakes // Journal of Geophysical Research. — 1977. — Vol. 82, no. 20. — P. 2981–2987. — https://doi.org/10.1029/jb082i020p02981

Lander A. V., Shevchenko N. A. and Matveenko E. A. An artifact in the Kamchatka earthquake catalog: study and elimination // Bulletin of Kamchatka Regional Association «Educational-Scientific Center». Earth Sciences. — 2019. — 1(41). — P. 85–90. — https://doi.org/10.31431/1816-5524-2019-1-41-85-90 — (In Russian).

Levina V. I., Lander A. V., Mityushkina S. V., et al. The seismicity of the Kamchatka region: 1962-2011 // Journal of Volcanology and Seismology. — 2013. — Feb. — Vol. 7, no. 1. — P. 37–57. — https://doi.org/10.1134/s0742046313010053

Melnikov Yu. Yu. A Software Package for Determining Earthquake Hypocenters in Kamchatka on a Computer // Vulkanologiya i Sejsmologiya. — 1990. — No. 5. — P. 103–112. — (In Russian).

Mityushkina S. V., Tokarev A. V., Raevskaya A. A., et al. Automatic processing of macroseismic information on Kamchatka earthquakes based on an Internet questionnaire // Problems of Comprehensive Geophysical Monitoring of the Russian Far East. Proceedings of the Third Scientific and Technical Conference. — Obninsk : GS RAN, 2011. — P. 376–380. — (In Russian).

Ogata Y. Statistical Models for Earthquake Occurrences and Residual Analysis for Point Processes // Journal of the American Statistical Association. — 1988. — Vol. 83, no. 401. — P. 9–27. — https://doi.org/10.1080/01621459.1988.10478560

Okada Y. Surface deformation due to shear and tensile faults in a half-space // Bulletin of the Seismological Society of America. — 1985. — Vol. 75, no. 4. — P. 1135–1154. — https://doi.org/10.1785/bssa0750041135

Pavlov V. M. and Abubakirov I. R. Algorithm for calculation of seismic moment tensor of strong earthquakes using regional broadband seismograms of body waves // Bulletin of Kamchatka Regional Association «Educational-Scientific Center». Earth Sciences. — 2012. — 2(20). — P. 149–158. — (In Russian).

Pinegina T. K., Ozerov A. Y., Tsvetkov V. A., et al. Tsunami from the Mw 8.8 Kamchatka Earthquake of 29 July 2025 on the East Coast of Kamchatka and the North Kuril Islands // Pure and Applied Geophysics. — 2026. — Vol. 183, no. 1. — P. 1–25. — https://doi.org/10.1007/s00024-025-03873-1

Saltykov V. A. Possible problems of evaluation of spatial-temporal features of earthquake catalog representativity: case study for the Kamchatka catalog of Geophysical Survey of RAS // Bulletin of Kamchatka Regional Association «Educational-Scientific Center». Earth Sciences. — 2019. — Vol. 3(43). — P. 66–74. — https://doi.org/10.31431/1816-5524-2019-3-43-66-74 — (In Russian).

Saltykov V. A. Aftershocks of the April 3, 2023, Mw 6.6 Vilyuchinsk Earthquake, Kamchatka // Izvestiya, Physics of the Solid Earth. — 2025. — Vol. 61, no. 6. — P. 925–937. — https://doi.org/10.1134/S1069351325700909

Senyukov S. L., Droznina S. Ya. and Droznin D. V. 15 years of the operational final regional earthquake catalog for Kamchatka and the Commander Islands // Proceedings of the Tenth All Russian Scientific and Technical Conference with International Participation “Problems of Integrated Geophysical Monitoring of Seismically Active Regions” (Petropavlovsk Kamchatsky, September 28 – October 4, 2025). — Petropavlovsk Kamchatsky : KB GS RAS, 2025. — P. 164–172. — (In Russian).

U.S. Geological Survey, ANSS Comprehensive Earthquake Catalog (ComCat). — 2026. — URL: https://earthquake.usgs.gov/data/comcat/ ; Accessed [April 10, 2026]. U.S. Geological Survey [online dataset].

Utsu T. Aftershocks and earthquake statistics (II): further investigation of aftershocks and other earthquake sequences based on a new classification of earthquake sequences // Journal of the Faculty of Science, Hokkaido University. Series VII (Geophysics). — 1970. — Vol. 3, no. 4. — P. 197–266.

Volfman Yu. M., Pustovitenko B. G. and Kolesnikova E. Ya. New results of the tectonophysical analysis of the focal mechanisms of earthquakes in the Crimean-Black Sea region // Scientific Notes of V.I. Vernadsky Crimean Federal University. Geography. Geology. — 2022. — Vol. 8, no. 4. — P. 163–206. — (In Russian).

Yunga S. L. On the mechanism of deformation of the seismically active volume of the Earth's crust // Izvestiya AN SSSR. Fizika Zemli. — 1979. — No. 10. — P. 14–23.